

Change of surface design of monopile
(Revised)

MASTER THESIS
MADS BAK-JENSEN
STRUCTURAL AND CIVIL ENGINEERING
AALBORG UNIVERSITY
JUNE 8TH 2018



AALBORG UNIVERSITY
STUDENT REPORT

The School of Engineering and Science
Structural and Civil Engineering
Thomas Manns Vej 23
9220 Aalborg Øst
<http://www.aau.dk>

Title:

Change of surface design of monopile

Project:

Master thesis

Project period:

February 2018 - June 2018

Project group:

Mads Bak-Jensen

Supervisors:

Søren Dam Nielsen

Johan Clausen

Editions: 1

Report pages: 66

Appendix pages: 13

Completed 8/6 2018

Synopsis:

In this report an analyses of a proposals to change the surface design of a monopile will be conducted, the surface design is suggested by Vattenfall. The suggestion is to change the surface from an exterior smooth to a jagged surface design. The problem statement for the project is: *Is it possible to save material for the monopile design when changing the surface design?*. To make the analysis a 3D model is set up for each surface design in PLAXIS 3D. To simplify the 3D model a 1D model is set up also for each surface design. To make sure that the simplified 1D models are showing identical results as the 3D models deformations and load-displacement curves will be compared. When a comparison of the surface design was conducted, the comparison showed that there was no significant difference between the two surface designs in respect to deformations using static analysis.

Preface

This report is conducted by a student that attend the 4nd semester of studies at Aalborg University as a part of the master program in Structural and Civil Engineering.

Prerequisites for reading the report is basic knowledge regarding Structural engineering.

Reading guide

This report is divided into two parts, the main part and the appendix. In the first part, the problem is introduced and analysed. The second part is connected to the first one by using references, where the theories and derivations are presented.

The axis through this report will be as Figure 1 shows. The coordinate system is the same even when referencing to theory names, eg. in the case with load-displacement curves where $p(y)$ will be the same as $p(u_x)$.

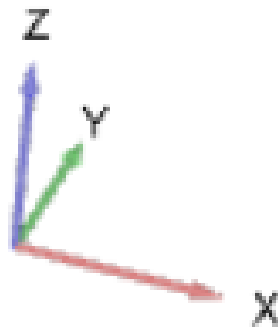


Figure 1. Coordinate system used.

Through the report source references in the form of the Harvard method will appear and these are all listed at the back of the report. References from books, homepages or the like will appear with the last name of the author and the year of publication in the form of [Author, Year]. They can furthermore appear with specific reference to a chapter, page, figure or table.

Figures and tables in the report are numbered according to the respective chapter. In this way the first figure in chapter 3 has number 3.1, the second number 3.2 and so on. Explanatory text is found under the given figures and tables. Figures without references are composed by the author.

Resume på dansk

I dette projekt vil et forslag om en ændring af hvordan overfladen af monopæle er designet blive fremstillet i håb om mulighed for at spare materiale. For at undersøge, om der er en mulighed for at spare materiale, vil der blive opstillet to 3D modeller for de forskellige design forslag. Modellerne vil blive moduleret i 3D finite element programmet PLAXIS. I et forsøg på at simplificere de opstillede 3D modeller vil der dernæst blive opstillet to 1D modeller. 1D modellerne vil blive sammenlignet med de beregnede flytninger og kurver baseret på flytninger fra 3D modellerne.

Forslaget om at ændre overflade designet er fremstillet af Vattenfall og går ud på at den normale glatte yderside af monopælen vil blive ændret til en takket overflade. Dette skulle gerne resultere i at materiale forbruget vil blive mindre for den takkede overfalde. Det takkede overflade design forventes at have en større skind friktion da den er mere ru end den glatte yderside.

Jordprofilen, monopælen simuleres at skulle være i, består af først to lag af løst lagret sand, som bliver efterfulgt af et lerlag. Efter lerlaget er der tre lag bestående af sand, hvor det midterste lag er løst lagret, mens de to andre er af middel lagret sand. Jordprofilen er en tænkt jordprofil og består kun af få parametre.

3D modellerne vil blive baseret på materiale modellen beskrevet af Mohr-Coulomb og vil derfor give en indikation på de effekter, som lastpåvirkningerne har på jorden omkring monopælen. Fra 3D modellerne vil der blive vist resultater i form af flytninger både vertikalt og horisontalt, der vil også blive lavet kurver baseret på de flytninger, som opstår i monopælen under de horisontale lastpåvirkninger. Modellerne vil blive sammenlignet på baggrund af de kræfter, som der skal til at opnå den samme flytning.

Fra de opstillede 1D modeller er der produceret flyttingskurver i form af $p-y$ og $t-z$ kurver. Derudover vil der blive vist $Q-z$ kurver, som beskriver den vertikale flytning af spidsen af pælen under vertikal last påvirkning. De respektive flytninger for de vertikale og horisontale last påvirkninger vil også blive bestemt.

I 1D modellerne er elementerne for den horisontale kraftpåvirkning modelleret som bjælke elementer med 4 frihedsgrader, mens elementerne for den vertikale lastpåvirkning er modelleret som stang elementer, som kun har to frihedsgrader.

Da modellerne er sammenlignet, kan det konkluderes, at resultaterne fra 3D modellerne og 1D modellerne viser de samme resultater.

For at se om det er muligt at spare materiale ved at ændre i overfalde designet er de to 3D modeller og de to 1D modeller sammenlignet. Ud fra disse modeller kan det konkluderes, at det tyder på at der ikke kan spares materiale. Da kurverne for designet med den glatte yderside viser, at de kraftpåvirkninger som forårsager den sammen flytning er meget højere end dem for designet med den taggede ydersider. Hvilket vil sige, at det design som bruges

nu, er det mest materiale besparende design.

Abstract in english

In this project a proposal for how the surface of monopiles alternatively could be designed with the possibility of reducing material costs. To investigate if it is possible two 3D models will be established, in the 3D finite element program PLAXIS, one model for each proposed design. In an attempt to simplify the 3D models two 1D models will be made. Furthermore, the models will be compared to the calculated displacements and the displacement curves.

The proposal of changing the surface design is given by Vattenfall and is about changing the exterior smooth surface of the monopile to a jagged surface. This change should result in reducing the material cost when the jagged surface is implemented. The jagged surface is expected to have a greater skin friction due to it being rougher than the smooth surface.

The soil profile in which the monopile is simulated, consists of two layers of loose sand followed by a layer of clay. After the clay layer there is three additional layers of sand where the middle layer is loose while the other layers are of medium density. The ground profile is a selected profile and consists of few parameters.

The 3D models are based on the material model described by Mohr-Coulomb and will therefore indicate the effect of the loads that the monopile has on the ground around the monopile. From the 3D models results are shown in the form of displacements both vertical and horizontal. Load-displacement curves are also made based on the displacements which occur in the monopile during loading.

From the 1D models, displacement curves in the form of $p-y$ and $t-z$ curves are produced. Furthermore, $Q-z$ curves will be presented, these describe the vertical displacement of the tip of the pile under vertical loading. The respective displacements for vertical and horizontal loads cases will also be determined.

In the 1D models the elements for the horizontal force is modelled as beam elements with four degrees of freedom per element while the vertical load is modelled as bar elements, which only have two degrees of freedom per element.

As the models are compared it can be concluded that the 3D and 1D models show the same results. To check the possibility for a reduction of material cost the two 3D models and the two 1D models are compared. From this comparison it can be concluded that it seems like there is a no valuable reduction. Since the curves of the design with the exterior smooth surface design show, that the forces causing the displacements are much higher than the forces causing the same displacements for the design with the jagged surface design. Which means that the design currently used is the most material-saving design.

Table of contents

Chapter 1 Introduction	1
1.1 Case description	1
1.1.1 Monopile Design	3
1.2 Problem statement	5
1.2.1 Limitations	5
1.3 Design parameters	6
1.3.1 Monopile	6
1.3.2 Soil	6
1.3.3 Loads	7
1.4 Methodology	8
Chapter 2 3D model	11
2.1 Model build up	12
2.1.1 Soil	12
2.1.2 Structure	14
2.1.3 Mesh generation	16
2.1.4 Phases for calculation	19
2.2 Results	19
2.2.1 Exterior smooth	19
2.2.2 Jagged	22
2.2.3 Comparison	24
Chapter 3 1D pile model	29
3.1 Winkler model	29
3.2 Statical systems	31
3.3 Load-displacement relationships	32
3.3.1 Axial resistance	32
3.3.2 Laterally loaded piles	36
Chapter 4 1D Finite Element Model	39
4.1 Input parameters	39
4.1.1 Soil	39
4.1.2 Monopile	40
4.1.3 Load	40
4.2 Model build up	40
4.2.1 Stiffness of the pile	41
4.2.2 Stiffness of the soil	41
4.2.3 Statical systems	41
4.2.4 Displacement curves	41
4.3 Results	41
4.3.1 Exterior smooth surface	41

4.3.2	Jagged surface	44
4.4	Comparison	47
Chapter 5	Conclusion	49
5.1	Comparison of calculation methods	49
5.2	Discussion	49
5.2.1	Focus	50
5.2.2	Loading type	50
5.2.3	Soil parameters	50
Bibliography		51
Appendix A	Monopile	53
Appendix B	Mohr-Coulomb	55
B.1	Yield condition	55
Appendix C	Elements for 3D model	57
Appendix D	Finite Element analyses	59
D.1	Establishment of stiffness matrix	60
D.1.1	Bar element	60
D.1.2	Beam element	61
D.1.3	Connecting elements	65

In this chapter the monopile design and the soil conditions will be described.

1.1 Case description

Because of the increasing demand for renewable energy the interests for design of wind turbines is increasing and because of this also the interests for the design of the monopile increases. Monopiles are the most common used foundation for wind turbines due to the easy installation in shallow to medium water depth. Monopiles are well suited for water depths ranging from 0-30m [4Coffshore, 2013].

Wind turbines are increasing in size when the matter in question is production of electricity, this leads to an increase in the diameter of of the wind turbine tower because the loads are increasing. This again leads to an increase in the diameter of the monopile this causes the material cost to increase with it.

A monopile is a simple structure design in which one large pile supports the wind turbine tower, either through a transition piece or directly. A transition piece is a transition section between the tower and the monopile. A transition piece is shown in Figure 1.6. The monopile is installed in the seabed at a sufficient depth. A monopile is typically a steel structure made of circular tubes and is normally fabricated in one piece [DNV GL AS, 2016].

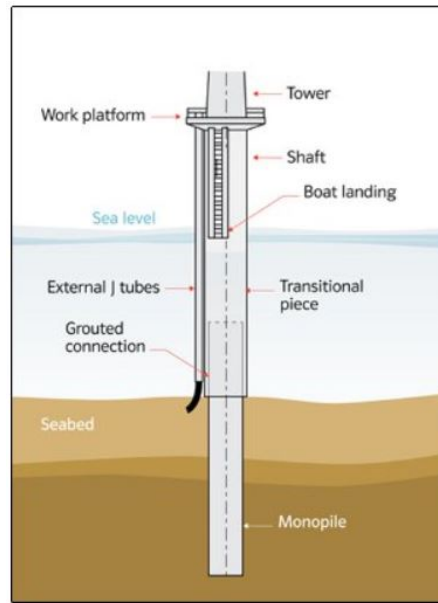


Figure 1.1. Monopile foundation [4Coffshore, 2013]

A monopile is produced of a number of circular tube sections welded together. The sections there are welded together can be seen in Figure 1.2.



Figure 1.2. Monopile sections welded together [Krabbendam, 4 January 2017]

If the transition piece is used it's typically equipped with appurtenances such as the platform where the boat is docking when the wind turbine is installed and when doing maintenance, some of these appurtenances can be seen on the transition piece in Figure 1.1. The monopile is typically installed before the transition piece is placed. The transition piece is typically also made of circular steel tubes and is also fabricated in one piece [DNV GL AS, 2016].

In an attempt to save material for the monopile a change in the surface design is proposed by Vattenfall. A sketch of traditional designs is shown in Figure 1.3, and the new design

proposal with a jagged surface, is shown in Figure 1.4. The basic thoughts for the proposed surface design is, if the monopile is made without eccentricities the loads transfer between the monopile sections are without torque transfer and therefore it should be possible to save material. This thought means that now the center line of the sections flange are aligned, this should give a better vertical down lead of the loads.

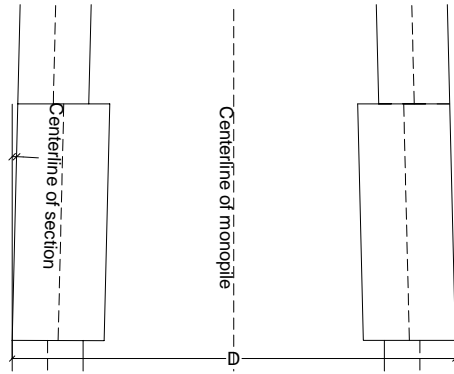


Figure 1.3. Scaled sketch of the connection for the exterior smooth surface.

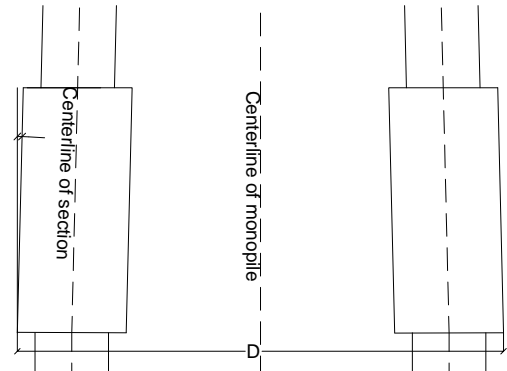


Figure 1.4. Scaled sketch of the connection for the jagged surface.

In this project the bearing capacity and the soil-structure interaction will be examined. If the new design and the currently used design are showing similar result or maybe even better results for the new surface design, there could be a possibility of saving material.

1.1.1 Monopile Design

The monopile should be designed to withstand loads which are static, cyclic and transient, without large vibrations or deformations in the platform. Some of the loads acting on the structure are illustrated in Figure 1.5. This also applies to the structural response of the piles [American Petroleum Institute, 2005].

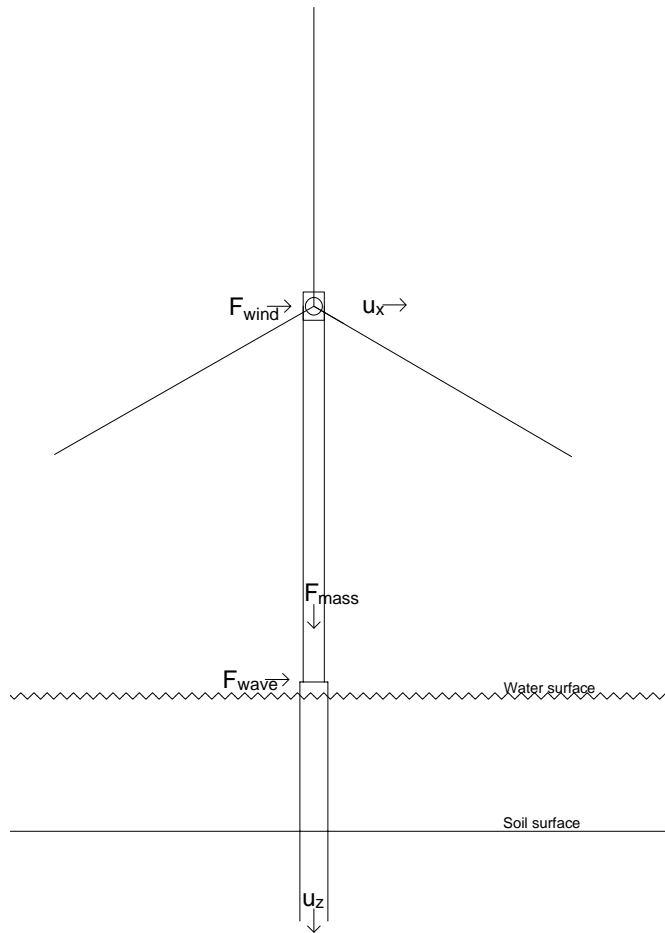


Figure 1.5. Sketch of the dominating loads on the monopile

Actual design

The design of the monopile is determined by Vattenfall, and two proposals for the design of the monopile are made. The traditional designs for the monopile has an exterior smooth surface, shown in Figure 1.3, and the new design proposal with a jagged surface is shown in Figure 1.4. The basic monopile design can be seen in Figure 1.6.

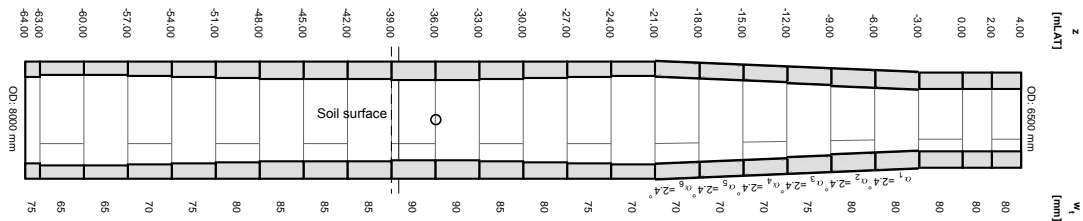


Figure 1.6. Monopile Design A bigger figure can be seen in Figure A.1.[Vattenfall, 2018]

For the exterior smooth surface a sketch of how the connection between the different sections are made is shown in Figure 1.3. As it can be seen in the figure the outer surface is smooth but the center line of the section flange isn't aligned, but the center line of the section is.

A sketch of the jagged surfaced monopile can be seen in Figure 1.4. Now are also the center line of the sections flange aligned.

To determine if there is a possibility for saving material if the surface design is changed, a 3D model for each surface design will be constructed. To simplify the 3D models 1D models for the respective surface design are made. The main reason for making the 1D models are that they are faster to run and it is easier to change the parameters in the 1D models than the 3D model. When the models are established the surface designs will be compared both in terms of model accuracy and the possibility of saving material.

1.2 Problem statement

The purpose of the project is to make an analysis if there is a possibility to save material during construction of the monopile if the surface design is changed from exterior smooth to a jagged surface design. To make this analysis a 1D finite element model is set up. To control this model a 3D model of the monopile is also constructed. The models are constructed in a way so the exterior smooth surface is examined first and then the jagged surface. The reason for this is that the jagged surface is the new design proposal made by Vattenfall and therefore the known model first has to work satisfactorily before the new design is examined.

The actual problem is

Is it possible to save material for the monopile design when changing the surface design?

To examine if there is a possibility to save material some finite element models, F.E.M., will be made to describe the load-displacements relationship which describes the soil effect on the pile depending on different load cases. The results from these models will be presented in form of curves and the total displacements. To validate these curves a 3D model is made and the results from the model will be compared with the results from the F.E.M..

1.2.1 Limitations

In this project the effect of scour and the dynamic effects from the environmental load will not be taken into account. The only environmental loads that will be considered is the wave and wind load.

The reason for not considering the scour effect is that the effect will be the same in both models for the surface design. Since the scour for this kind of structure often will be simulated as a hole around the construction, this hole is depending on the diameter of the construction and will therefore be equal for the two surface designs.

The slope of the elements, shown in Table 1.1 will also not be taken into account in this project. The reason for not considering the slopes is that they are above the soil surface. This means that the elements there was supposed to have a slope will be modelled with the average diameter of the element section and vertical element flange.

1.3 Design parameters

The design parameters for this project are given by Vattenfall and will be presented in the following.

1.3.1 Monopile

The parameters for the designs of the monopile is presented in Table 1.1. How the diameter and the slope are measured is shown in Figure 1.3 for the exterior smooth surface and in Figure 1.4 for the jagged surface.

Depth point [m]	Depth [m]	Exterior smooth			Jagged		
		Diameter [mm]	Slope, α [deg]	Thickness [mm]	Diameter [mm]	Slope, α [deg]	Thickness [mm]
4.00	42.50	6500	0	80	6500	0	80
2.00	40.50	6500	0	80	6500	0	80
0.00	38.50	6500	0	80	6500	0	80
-3.00	35.50	6500	2.4	80	6500	2.4	80
-6.00	32.50	6750	2.4	80	6746	2.4	80
-9.00	29.50	7000	2.4	75	6992	2.4	75
-12.00	26.50	7250	2.4	70	7243	2.4	70
-15.00	23.50	7500	2.4	70	7493	2.4	70
-18.00	20.50	7750	2.4	70	7744	2.4	70
-21.00	17.50	8000	0	70	7995	0	70
-24.00	14.50	8000	0	75	8000	0	75
-27.00	11.50	8000	0	80	8005	0	80
-30.00	8.50	8000	0	85	8010	0	85
-33.00	5.50	8000	0	90	8015	0	90
-36.00	2.50	8000	0	90	8015	0	90
-38.50	0.00	8000	0	90	8015	0	90
-39.00	-0.50	8000	0	85	8010	0	85
-42.00	-3.50	8000	0	85	8010	0	85
-45.00	-6.50	8000	0	85	8010	0	85
-48.00	-9.50	8000	0	80	8005	0	80
-51.00	-12.50	8000	0	75	8000	0	75
-54.00	-15.50	8000	0	70	7995	0	70
-57.00	-18.50	8000	0	65	7990	0	65
-60.00	-21.50	8000	0	65	7990	0	65
-63.00	-24.50	8000	0	75	8000	0	75
-64.00	-25.50	8000	0	75	8000	0	75

Table 1.1. Monopile parameters

1.3.2 Soil

The soil parameters for this project are given by Vattenfall in a design report, [Vattenfall, 2018]. It is a fictitious soil profile there is used for this project. The soil profile consists

of first two layers of sand and then a layer of clay followed by three layers of sand. The parameters for the soil profile is presented in Table 1.2.

Soil layer	Depth [m]	γ' [kN/m ³]	s_u [kPa]	φ [deg]	G_0 [kPa]	ε_{50} [%]
Sand 1	-38.5, -44.5	10.50	-	35.5	20	-
Sand 2	-44.5, -49.5	11.00	-	39.0	20	-
Clay 1	-49.5, -51.0	10.00	62.50	-	20	1.5
Sand 3	-51.0, -55.5	11.00	-	40.5	20	-
Sand 4	-55.5, -72.5	11.00	-	38.0	20	-
Sand 5	-72.5, -88.5	11.00	-	40.5	20	-

Table 1.2. Soil parameter

1.3.3 Loads

The load acting on the monopile is the mass of the wind turbine tower and the transition piece. Also the environmental loads are acting on the structure, some of these loads are the wind and wave load. How these loads are effecting the construction is sketched on Figure 1.7

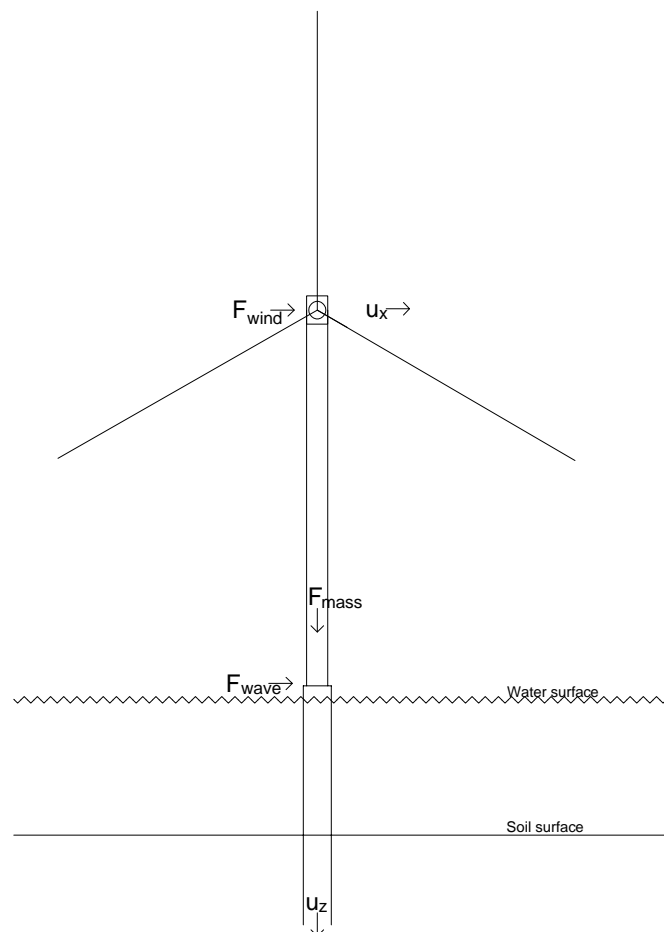


Figure 1.7. Sketch of the dominating loads on the monopile

The mass of the wind turbine tower and the transition piece, and extra mass is presented

in Table 1.3. The mass of the tower itself is 343.4 t, and the mass of the transition piece itself is 192.6 t [Vattenfall, 2018].

Height [m]	Mass [t]	Description
110.8	478.30	Nacelle
108.3	1.56	Distributed mass
107.1	3.04	Distributed mass
102.1	25.00	Distributed mass
74.7	2.54	Distributed mass
74.6	2.54	Distributed mass
46.2	4.93	Distributed mass
46.0	4.93	Distributed mass
35.2	50.00	Distributed mass
20.0	20.00	Ext platform
19.8	1.50	UW platform
16.0	15.00	SWG platform
16.0	1.41	External res
12.0	9.00	Boat landing
4.0	23.00	MP TP Flange
3.0	7.26	AT platform
2.0	90.00	Skirt

Table 1.3. Extra mass contributions on tower

When modelling the environmental loads the load will be simulated as a forced displacement at the seafloor. From this displacement the forces acting on the seafloor level will be determined and used to create the graphs which will be compared.

As mentioned will the dynamic load effect of the environmental loads not be considered in this project.

1.4 Methodology

When the problem and all the parameters are presented the next is to solve the problem, this will be done in the following manner.

First the two 3D models will be established. How these models are established are described in chapter 2 the results from this models will also be presented. The results will be presented in form of load-displacements curves.

To simplify the 3D model 1D models will be created. The theory behind the 1D models and the factors used for the 1D models are described in chapter 3.

When the theory for the 1D models are described, how the 1D models are build will be presented, this is done in chapter 4. When model build up is described the results from the different surface designs will be presented and compared. The results will be presented in form of load-displacements curves.

When the results from the different model are presented the verification of the 1D models

can be made and a conclusion can be made. This is done in chapter 5. Based on the conclusion a discussion of the results will be made. In the discussion there will be reflected on what there went well and what could have been done differently and the effects of this.

3D model 2

In this chapter the 3D finite element models will be described. The 3D models are used to investigate if there is a possibility to save material for the monopile if the surface design is changed. The program used for these 3D models is PLAXIS 3D.

In order to investigate if there is a possibility to save material during the construction of the monopile if the surface design is changed as described in section 1.1.1, finite element, FE, models are established.

First it will be described how the FE model is build up in PLAXIS. This is done in the same order as the model is build in the program, so it is possible to build the models again if it is wanted. When the model build up is described the results of the models will be presented and the results from the exterior smooth surface and the ones for the jagged surface will be compared.

The primary purpose of the 3D model are to examine if there are potential for a reduction of material costs when changing the surface design. For this purpose two models are set up and the results of these will be compared. The results of the models will be presented as load-displacement curves, in which the displacements are predefined. A sketch of the how the models will be build are shown in Figure 2.1. From the known displacement, δ , the forces necessary to force it, will be determined and these forces will be compared.

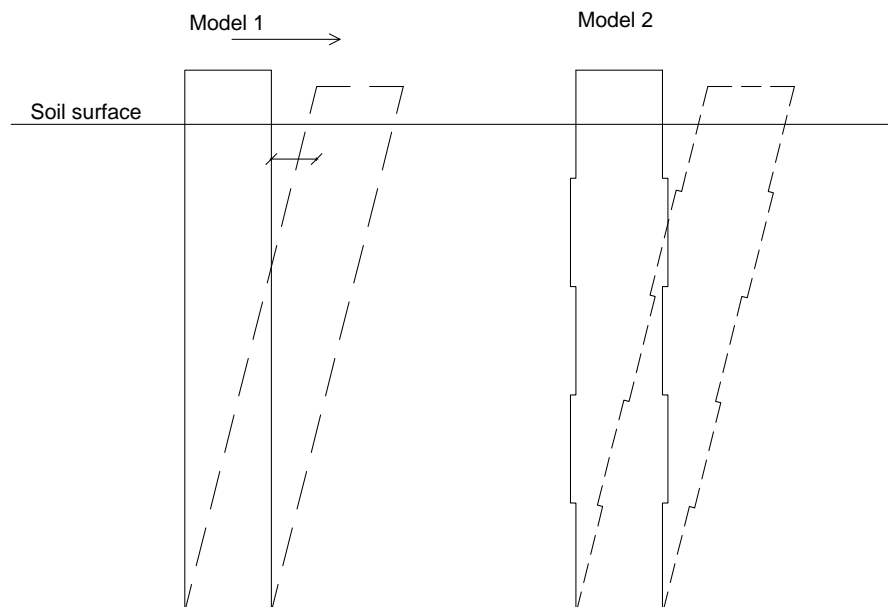


Figure 2.1. Sketch of the models.

The analytical bearing capacity is determined in the same manner as the total resistance, described in equation (3.2). The total resistance have to be larger than the loads acting on the monopile.

2.1 Model build up

To make a numerical analyse in PLAXIS 3D, many considerations have to be taken into account, these considerations will be described in the following.

Most of the input parameters are the same for both models, shown in Figure 2.1. Therefore, the parameters will be presented in the same section. The only parameter that is changing is the diameter for the monopile elements.

The first there have to be made in the PLAXIS model is determination of the model size. For this model the x axis is chosen to 100 m, the y axis is chosen to 50 m and the z axis is chosen to 50 m, a sketch of the model is shown in Figure 2.2. The reason for choosing to give the model this size is to avoid the influence from the boundaries. To make sure that the boundaries don't influence the results a color plot can give an indication. This indication could be if the displacement is hitting the boundary. It is only necessary to model the half of the monopile because the monopile and the forces acting are symmetrical around the x axis in Figure 2.2.

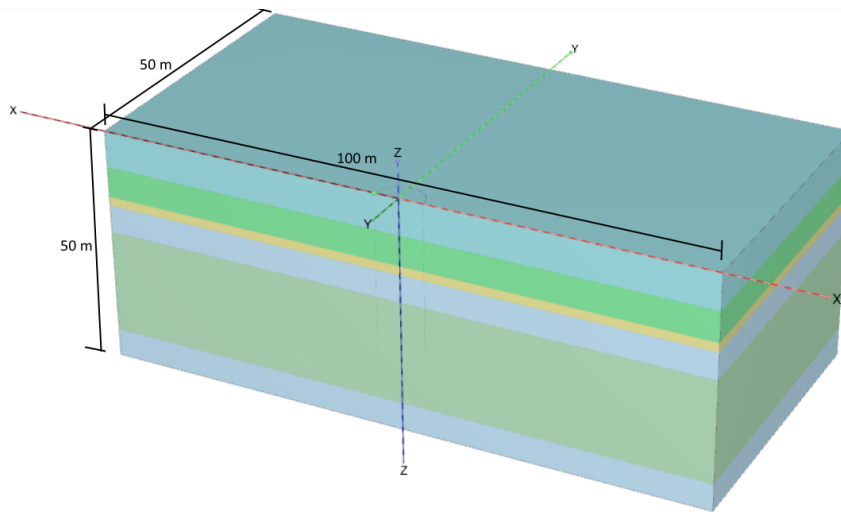


Figure 2.2. Sketch of the model.

2.1.1 Soil

When the model size is set the soil profile can be established by creating a borehole. In the borehole the information from Table 1.2 are used and the head is set to 38.5 m. The head define where the water pressure is zero, in this case the water surface is placed 38.5 m above the soil surface. The soil profile is shown in Figure 2.3 and the parameters used are explained in the following.

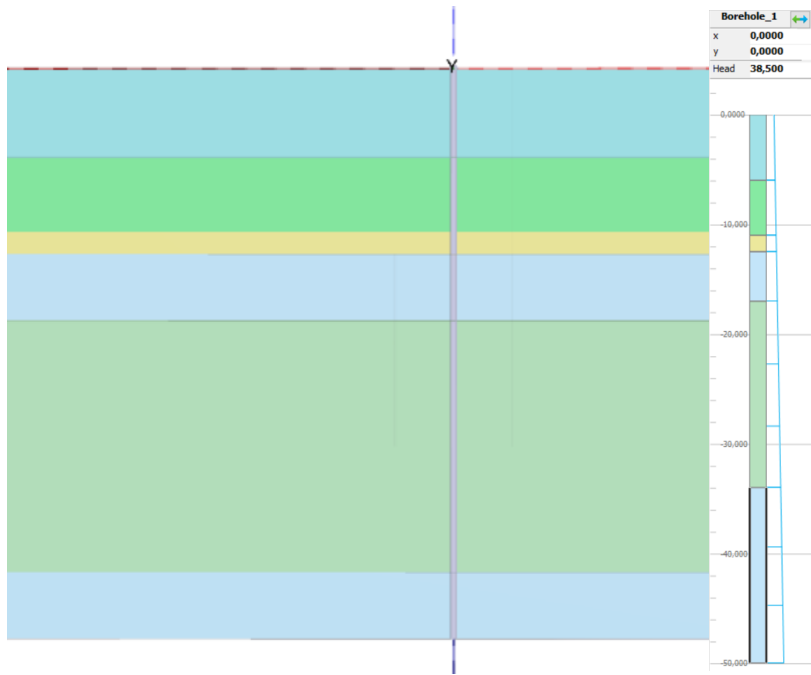


Figure 2.3. Soil profile for the models.

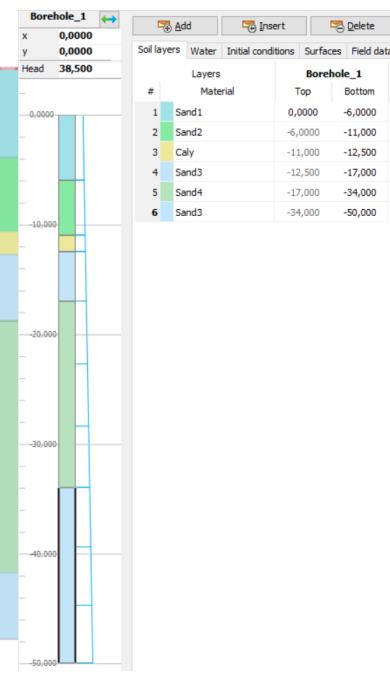


Figure 2.4. .

The soil parameters used for the model depends on the material model used. For these models the material model used is the Mohr-Coulomb failure criterion. The main reason for choosing this material model is that it is fast and with few input parameters and these models are only the start of a larger examination if it is possibly to save material when changing the surface design. The results will be compared with the result from the 1D FE models which is the displacements and the displacement curves, determined from the PLAXIS models, if these are similar, it indicates that the 1D models give the correct results.

The parameters used in the models are the soil unit weight, Poisson's ratio, initial shear modulus, undrained shear stress and the friction angel. These parameters for each soil layer are presented in the following tables, Table 2.1 for the drained soil layers and Table 2.2 for the undrained soil layers. When choosing the initial shear modulus the stiffness of the soil will be higher than in the reality because soils shear modulus is chancing when the soil is loaded. The reason for choosing the initial shear modulus, is that the error will be the same in all models and it is the value there is available for this project.

Soil layer	Depth [m]	γ' [kN/m ³]	ν [-]	G_0 kN/m ²	s_u [kN/m ²]	ϕ [deg]
Sand	0.0 - -6.0	10.5	0.33	20000	0	35.5
Sand	-6.0 - -11.0	11.0	0.35	20000	0	39.5
Sand	-12.5 - -17.5	11.0	0.35	20000	0	40.5
Sand	-17.5 - -34.0	11.0	0.34	20000	0	38.0
Sand	-34.0 - 50.0	11.0	0.35	20000	0	40.5

Table 2.1. Drained parameters for PLAXIS models

Soil layer	Depth [m]	γ' [kN/m ³]	ν [-]	G_0 [kN/m ²]	s_u [kN/m ²]	ϕ [deg]
Clay	-11.0 - -12.5	10.0	0.20	20000	62.50	-

Table 2.2. Undrained parameters for PLAXIS models

In Table 2.2 the depth is measured from the soil surface, γ' is the effective soil unit weight, ν is Poisson's ratio, which is estimated from Portali [2018], G_0 is the initial shear modulus of the soil, s_u is the undrained shear stress and ϕ is the friction angle. The dilation angle is assumed to be equal to zero, $\psi = 0$. Young's modulus, E , is determined from $E_0 = 2G_0(1 + \nu)$, which in this case will be the initial Young's modulus. Poisson's ratio for the undrained clay may be valued too low as it normally valued to 0.5 and in PLAXIS to 0.45.

Another parameter to be determined is the interface strength reduction factor R_{inter} . The surrounding soil's interfaces for real soil-structure interaction is weaker and more flexible, therefore R_{inter} should be less than one. A suitable value for R_{inter} is recommended to be 2/3 by PLAXIS [2017].

2.1.2 Structure

When the soil profile is created, the monopile can be constructed.

Section construction

The monopile is constructed as a number of sections. To create each section the first is to create a polycurve. To create the polycurve the segment type is chosen to *arc* and it should have a relative start angle at 90°, then set the wanted radius and then set the segment angle to 180°. The polycurve is set to start at (x,y,z) where x is the outer radius of the monopile section, y is, in this case, always set to 0, z is the depth for the top of the element. The radius for this polycurve is the outer diameter of the monopile section, the dimensions for the monopile is from Table 1.1, but the information needed to create the polycurves is shown in Table 2.3. When the first polycurve is made another polycurve is created. This polycurve is set to start at the inner radius of the monopile section.

Depth [m]	Exterior smooth			Jagged		
	Outer diameter [mm]	Thickness [mm]	Inner diameter [mm]	Outer diameter [mm]	Thickness [mm]	Inner diameter [mm]
0	4000	90	3910	4008	90	3918
-0.5	4000	85	3915	4005	85	3920
-3.5	4000	85	3915	4005	85	3920
-6.5	4000	85	3915	4005	85	3920
-9.5	4000	80	3920	4003	80	3923
-12.5	4000	75	3925	4000	75	3925
-15.5	4000	70	3930	3998	70	3928
-18.5	4000	65	3935	3995	65	3930
-21.5	4000	65	3935	3995	65	3930
-24.5	4000	75	3925	4000	75	3925

Table 2.3. Section parameters

When the two polycurves are created, as in Figure 2.5, two polylines is made to combine the two polycurves, one in each end. When the polylines is combined, a surface is created as shown in Figure 2.6. Then the surface is extruded to the wanted depth, this create a volume which is describing the monopile section.

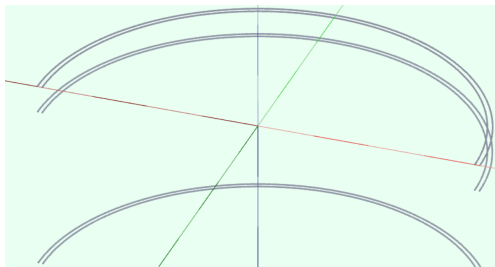


Figure 2.5. Polycurves describing the edge of the elements.

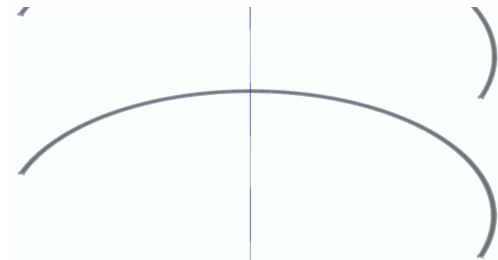


Figure 2.6. Surface between the polycurves.

Combining section

When all the sections are created the sections are selected and combined. Now all the sections are combined into one section, then the section is merged to the surrounding surfaces.

To be able to simulate the loading of the monopile the section is made to a rigid body. This assumption is made to simulate the load of the pile with a predefined displacement. This displacement will be presented and described later. The assumption of making the monopile as a rigid body is a fair assumption, because the monopile has a much higher stiffness than the surrounding soil. If the monopile is modelled as volumes with the material parameters as steel and as a linear elastic material, PLAXIS gives an error message telling that the "soil body seams to collapse" even if the monopile isn't loaded. Therefore, the monopile is modelled as a rigid body. This assumption can have an effect when comparing the 3D models with the 1D models. This can lead to displacements for the 1D models

higher than for the 3D models, as the monopile in the 1D models are simulated as linear elastic material.

2.1.3 Mesh generation

To generate the mesh for the models the coarseness has to be chosen. To choose a sufficient coarseness of the mesh a convergence analysis is made and the result is shown in Figure 2.7. The coarseness is determining the amount of elements used to described the models. To model the monopile the local coarseness is set to 0.1, the local coarseness generate a more dense mesh around the monopile which can describe the jagged surface on the monopile. This local coarseness is also effecting the amount of elements which describe the model.

The elements for the model are volume elements, this mean that the soil volume is modelled with 10 node tetrahedral elements [PLAXIS, 2018b]. This element type is described further in Appendix ???. The model is described with 93981 elements of this type.

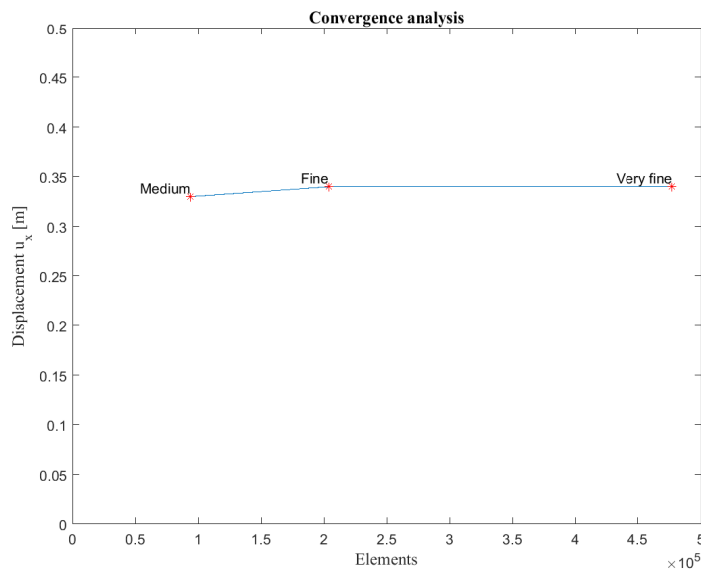


Figure 2.7. Convergence analysis for mesh coarseness.

Figure 2.7 consist only of three points, this is because PLAXIS cannot generate the mesh for a coarser mesh than the one called medium and the displacements do not change from fine to very fine on the graph. The coarseness of the mesh is based on the convergence analysis shown in Figure 2.7 and is chosen to medium.

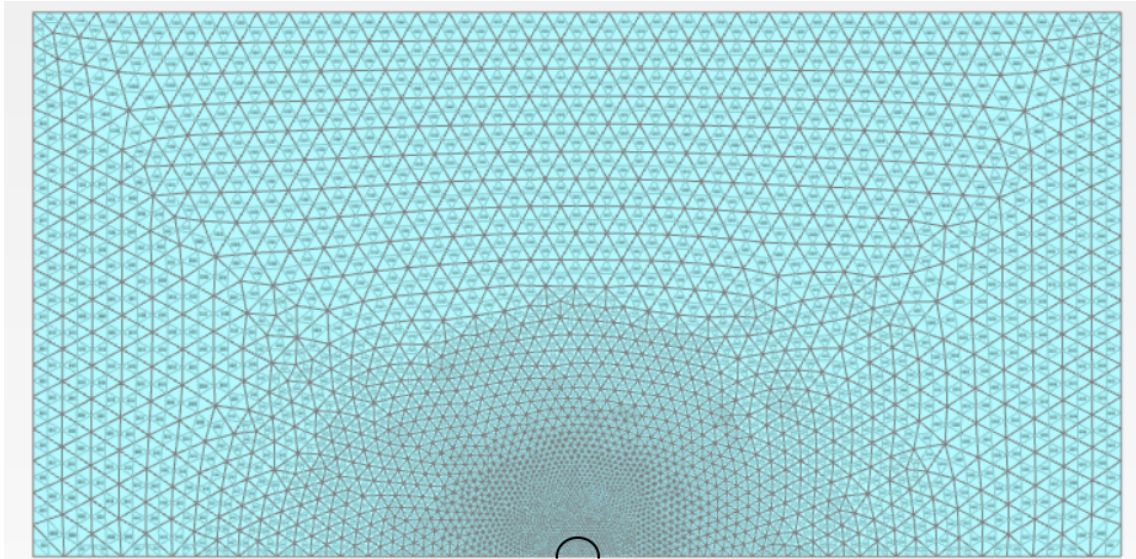


Figure 2.8. Mesh seen from above.

Figure 2.8 shows the mesh of the model seen from above. As seen in the figure the mesh is more fine around the monopile and close to the boundaries the mesh is becoming less fine. A close up of the mesh around the pile is shown in Figure 2.9.

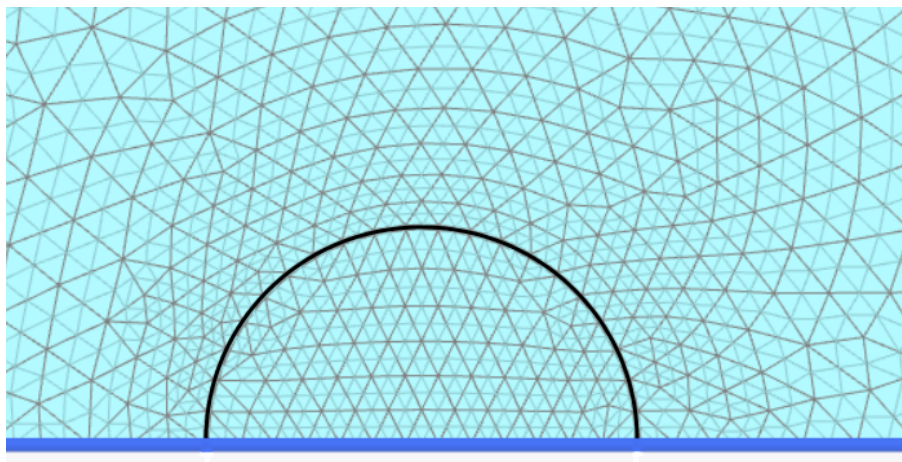


Figure 2.9. Close up of the mesh around the monopile seen from the top of the model.

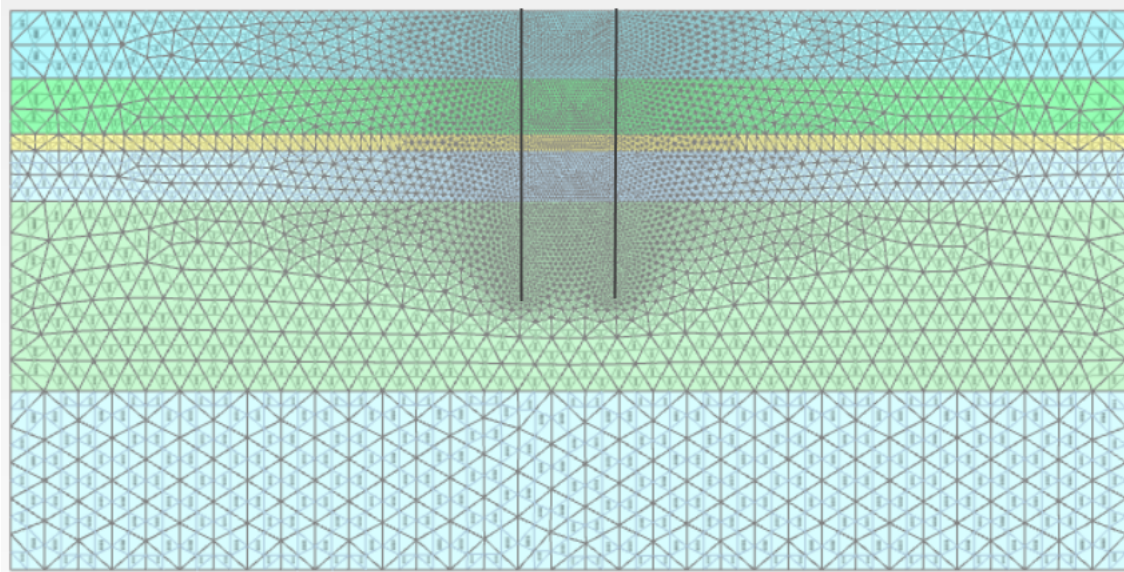


Figure 2.10. Mesh seen from the front of the model.

Figure 2.10 shows the mesh for the model seen from the front. Again the mesh is more fine around the monopile and becomes less fine close to the boundaries. A close up of the mesh around the monopile seen from the front is shown in Figure 2.11.

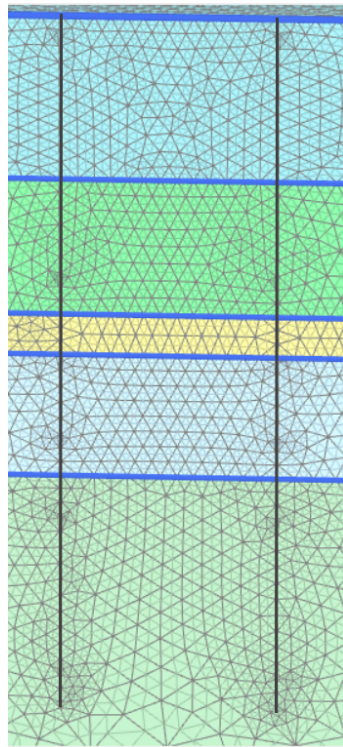


Figure 2.11. Close up of the mesh around the monopile seen from the front of the model.

When the mesh is generated the nodes of special interest are pointed out, these points could be where the soil layer is changing and another interesting point is in the middle of each element. For this project is the point chosen the point the location where the

displacement is added.

2.1.4 Phases for calculation

To perform the calculations for the models there are made phases. Each phase represent a different load scenario, the first phase is the initial conditions, the second phase is installation of the pile, which is modelled as wished in place, next phases are the different load cases.

The loads for the models are determined from the masses presented in section 1.3.3. The load for each phase is determined as follows. The axial load acting on the monopile is

$$Q = (m_{tower} + m_{TP} + m_{pile}) g = 1867 \text{ kN} \quad (2.1)$$

The axial load is then changed to a surface load, which is applied on the top of the monopile. This surface load is applied in all the phases of the simulation for the laterally loaded pile.

The lateral loads are determined from the prescribed displacement. The magnitude of the prescribed displacement is depending on when the soil body fails. This is seen from the load displacement curves when the displacement increase without increase of the forces.

The prescribed displacement are set to effect the monopile at its edge furthest to the left, which means at the point located at $(x,y,z)=(-4.0,0.0,0.0)$. The location of this point is shown in Figure 2.12.

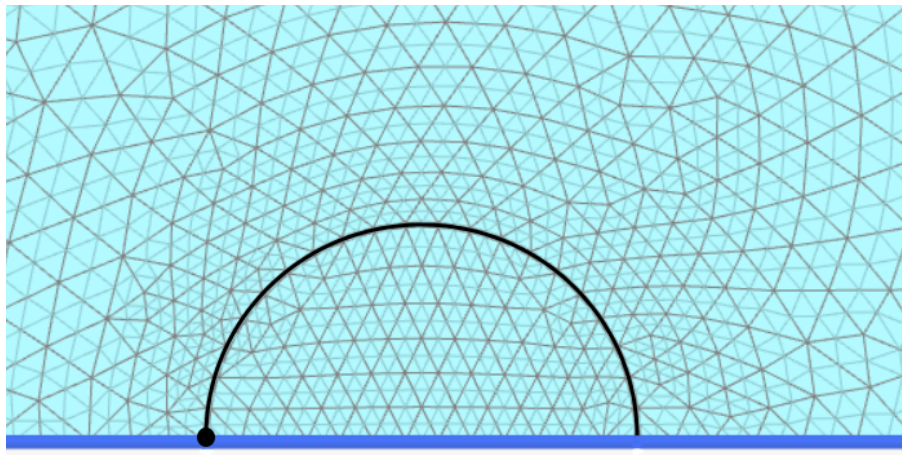


Figure 2.12. Location for the prescribed displacement.

2.2 Results

The results from the 3D model will be presented in the following. The results will be shown for one surface design at a time and then a comparison will be made.

2.2.1 Exterior smooth

The total displacement is illustrated in Figure 2.13 as a color plot and as a deformed mesh in Figure 2.14. The curves shows the total displacements and the forces acting in the

direction of the x-axes. The force shown is the force causing the primary displacement. The forced displacement for the colour plot in Figure 2.13 and the deformed mesh in Figure 2.14 is two meters.

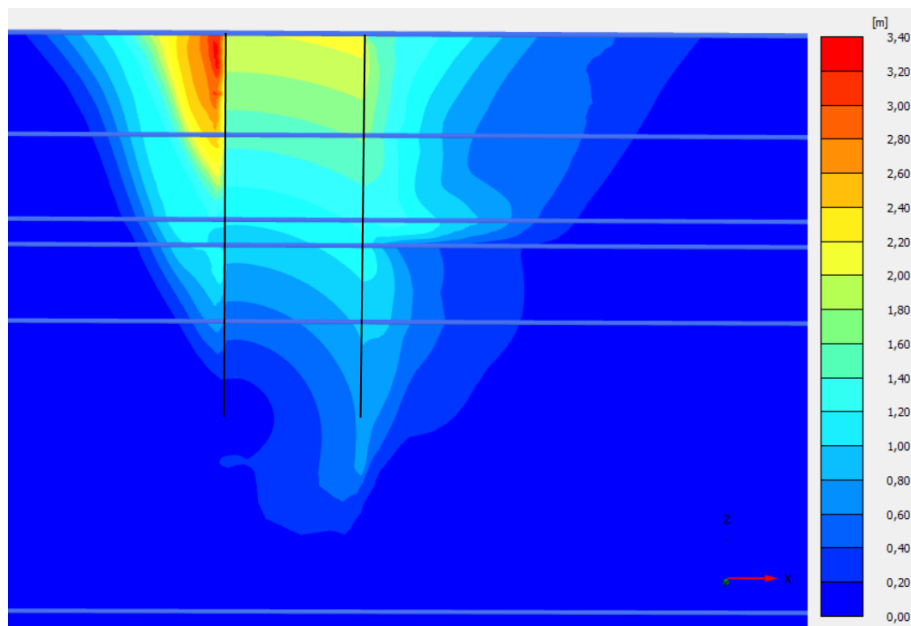


Figure 2.13. Colour plot of the displacement.

The color plot in Figure 2.13 is illustrating the displacement of the monopile. This color also indicate that the model size is big enough so the boundaries doesn't influence the displacements because the displacements are zero at the boundaries. It is seen that the displacement has linear variation along the pile, this is illustrated on Figure 2.13 with the colours at the figure. The value each colour are representing is also shown in the figure. The figure also shows that there is no displacement at the end of the pile in the side where the forced displacement is added.

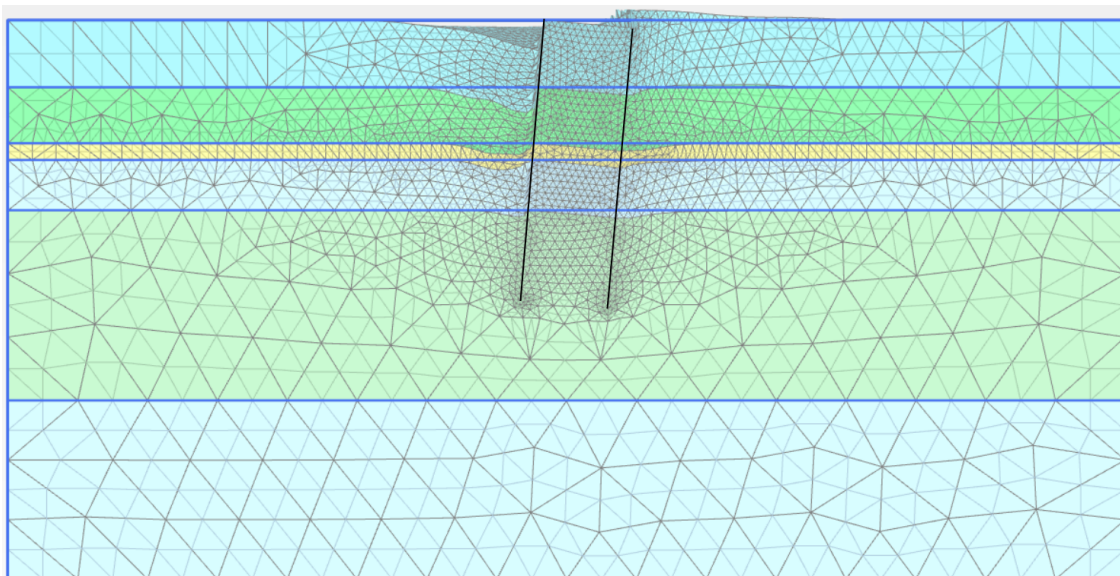


Figure 2.14. Deformed mesh.

From the deformed mesh in Figure 2.14 it is seen that the monopile push the soil up at the opposite side of the loading.

The load-displacement curves for the exterior smooth surface design is shown in Figure 2.15.

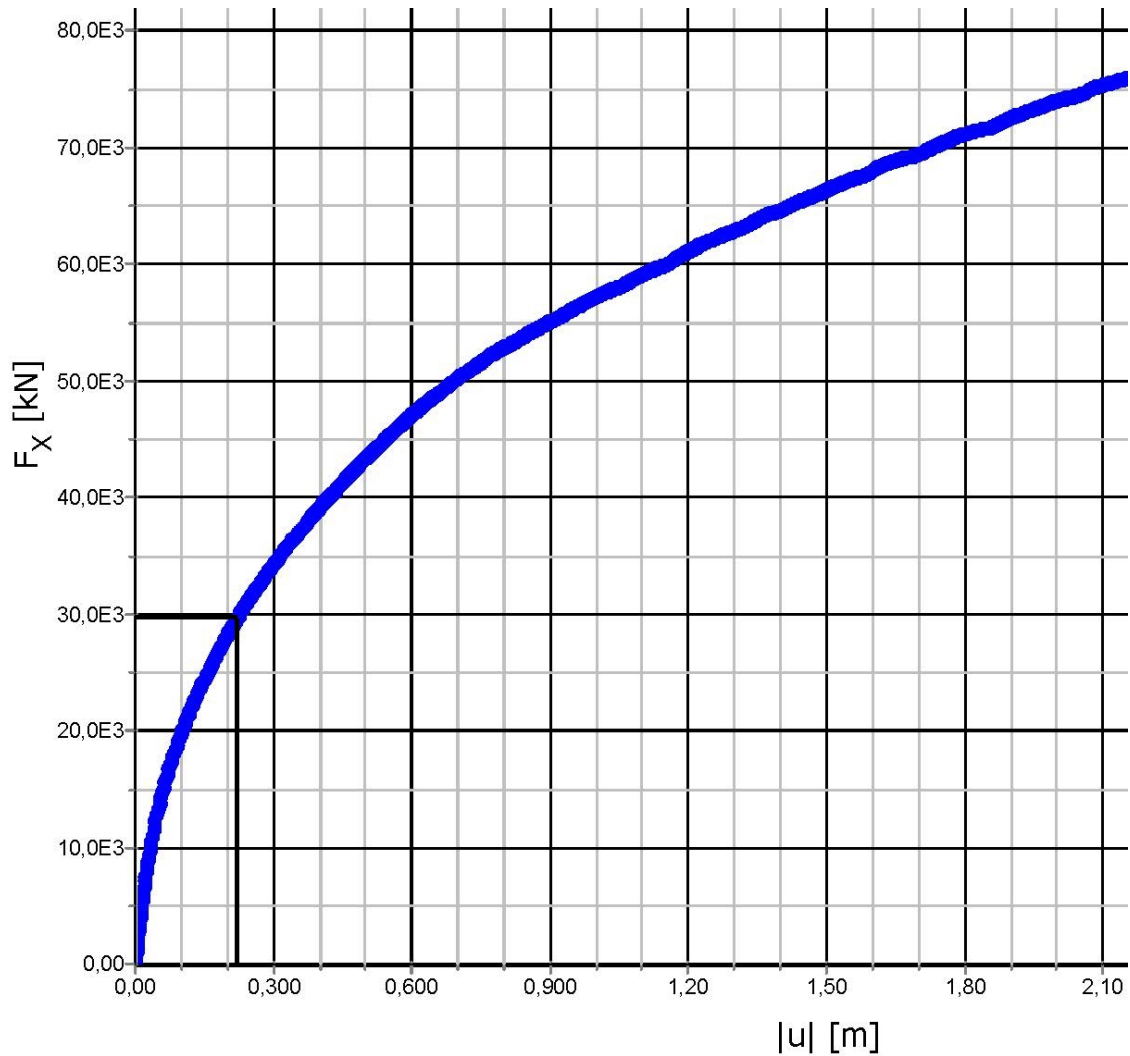


Figure 2.15. Load-displacement curve.

From the load-displacement curve the force necessary to cause the displacement can be seen and the results are shown in Table 2.4. Phase 1 is installation of the pile and there is therefore no displacement prescribed. Phase 2 have a horizontal prescribed displacement.

In Figure 2.15 the serviceability limit state, SLS, is illustrated as the black line and its results are also shown in Table 2.4. SLS is determined as DNV GL AS [2016] describe it. Which means that the allowed angle of vertical displacement equal to $0,50^\circ$ is the maximum the monopile can displace to comply with the SLS requirement. The vertical displacement there is allowed is in this case determined by simple triangle calculations, because the monopile is modelled as a rigid body. Therefore, the allowed displacement can

be determined from the rotation point and the angle of vertical displacement. This gives an allowed displacement on 0.22 m for the exterior smooth surface design.

Phase	Prescribed displacement	Total displacement	Force
Phase 1	0.00 m	0.015 m	0kN
Phase 2	2.0 m	2.02 m	74196 kN
SLS	0.00 m	0.22 m	29563 kN

Table 2.4. Results for the surface design.

The force in Table 2.4 is the force necessary to accumulate the prescribed displacement. The different of the prescribed displacement and the total displacement is that the total displacement also included the displacement caused by the surface load.

2.2.2 Jagged

As for the exterior smooth surface design the total displacement for the jagged surface design is illustrated in Figure 2.16 as a color plot and as a deformed mesh in Figure 2.17.

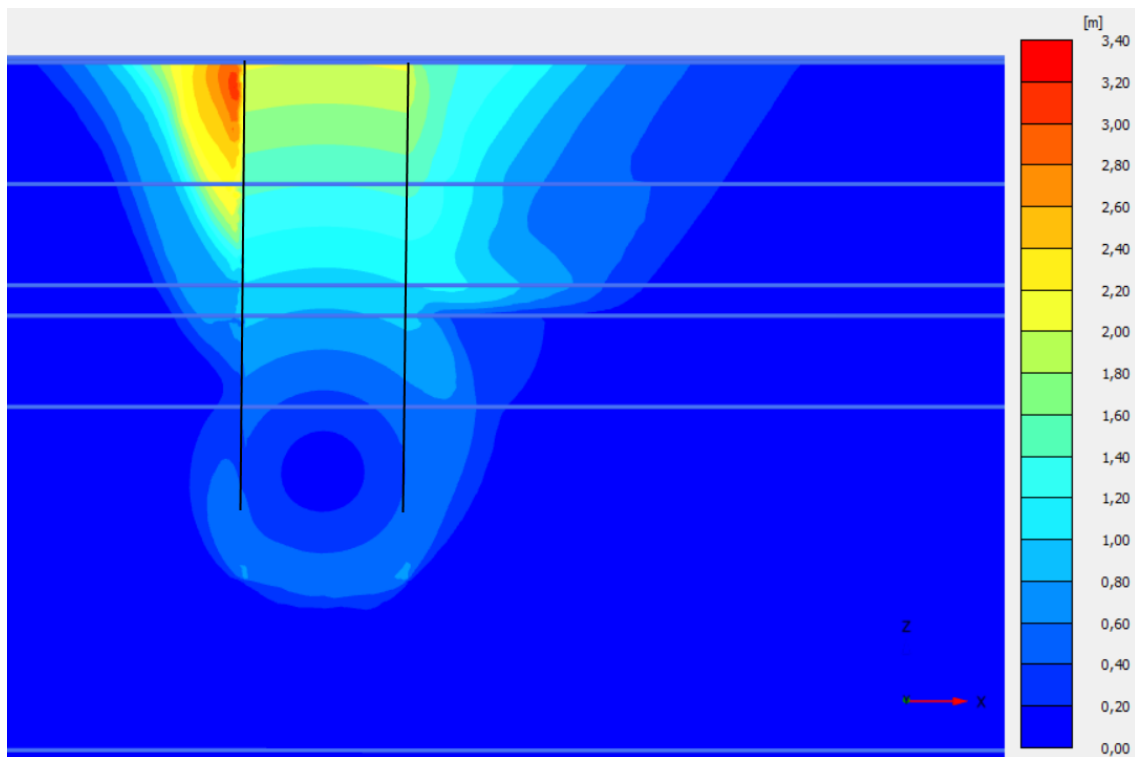


Figure 2.16. Displacement color plot.

From the displacement plot in Figure 2.16 it seen again that the model size is big enough so the boundaries doesn't influence the displacements, because the displacements are zero at the boundaries. It is also seen that the displacement has linear variation along the pile, but in this case there is a change in the displacement near the end of the pile. It looks like that the end of the pile is rotating around a point higher up than the end of the pile, this gives displacements at the end of the pile.

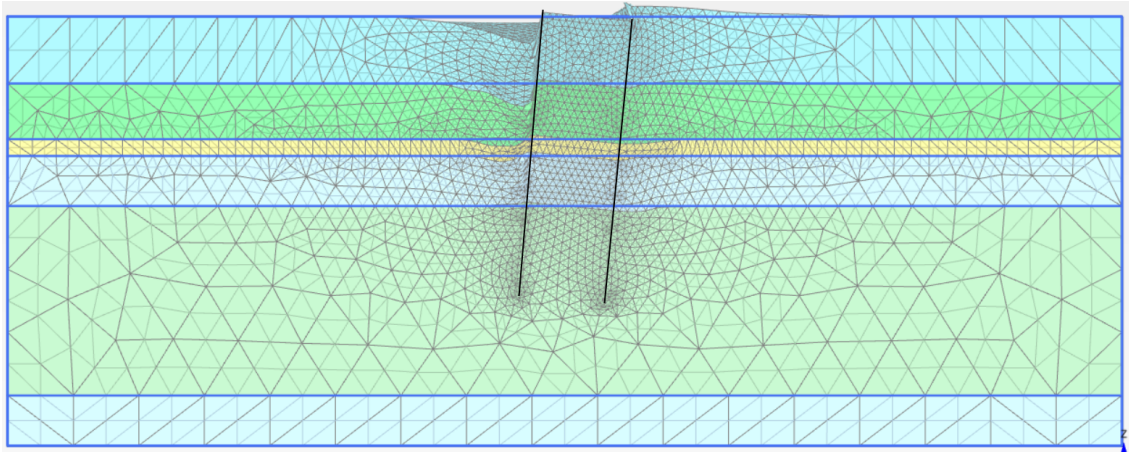


Figure 2.17. Displacement plot.

From the deformed mesh in Figure 2.17 it is seen that the monopile push the soil up at the opposite side of the loading.

The load-displacement curves for jagged surface is shown in Figure 2.18.

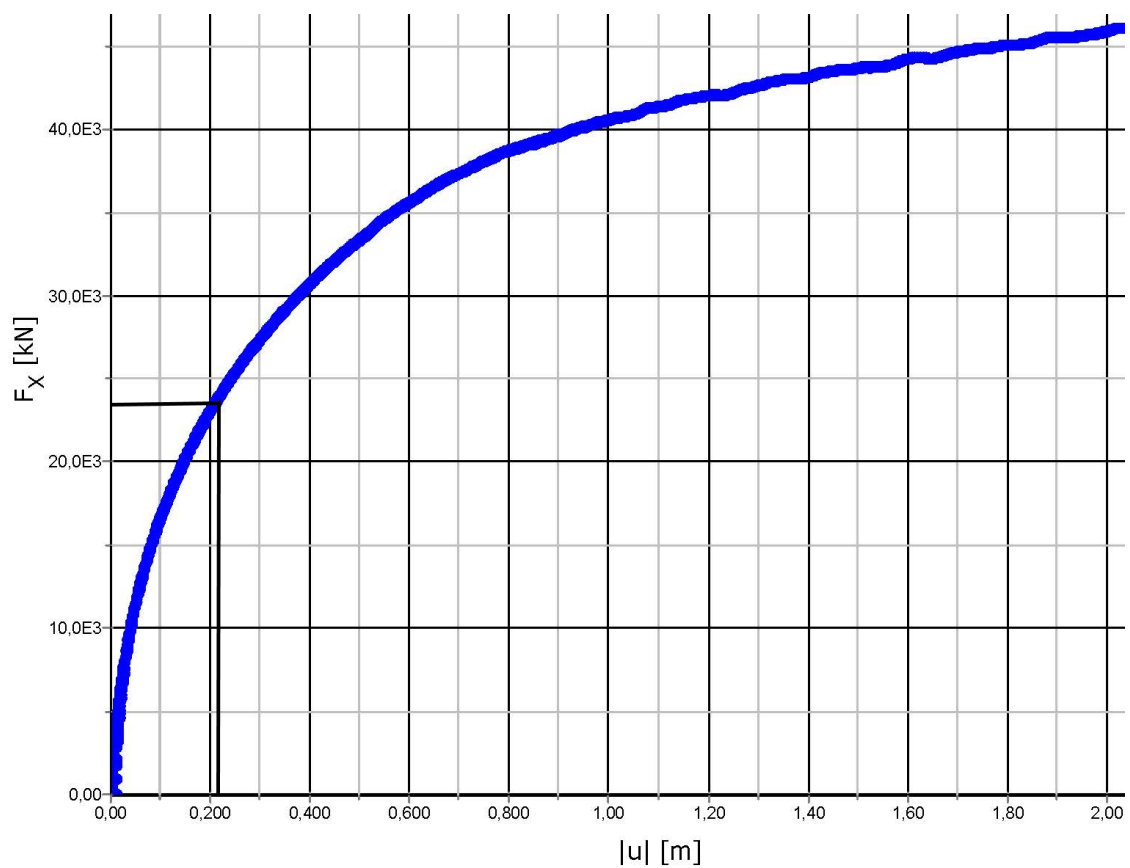


Figure 2.18. Load-displacement curves.

From the load-displacement curves in Figure 2.18 the force necessary to cause the displacement is shown in Table 2.5. Again the allowed displacement, according to SLS,

can be determined from the rotation point and the angle of vertical displacement. in This case is the allowed displacement 0.21 m.

Phase	Prescribed displacement	Total displacement	Force F_x
Phase 1	0.00 m	0.013 m	0kN
Phase 2	2.00 m	2.04 m	46005 kN
SLS	0.00 m	0.21 m	23602kN

Table 2.5. Results for the surface design.

In Figure 2.18 is the SLS again shown as a black line and the results is shown in Table 2.5. The allowed displacement is determined as in equation ?? and the result is 0.00 m

2.2.3 Comparison

When comparing the two surface designs the load-displacement curves for each phase will be examined individually. This is done to examine whether there are any difference between the surface designs both in the serviceability limit state and in the ultimate limit state or if there is a pattern in the curves.

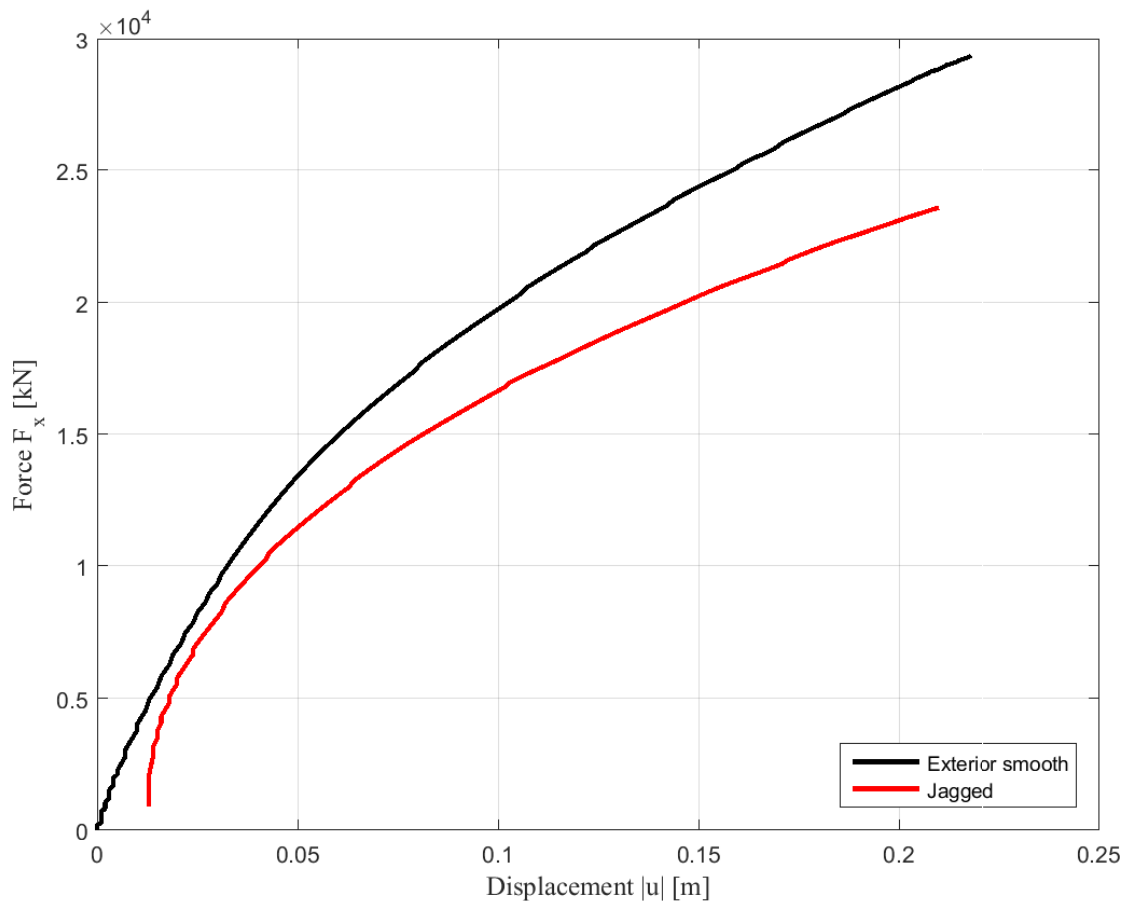


Figure 2.19. Load-displacement curves whit a forced displacement on 0.22 m.

Figure 2.19 shows the load-displacement curves whit a forced displacement on 0.22 m, it is showing an unexpected result. The graphs are showing the opposite of what was expected,

it shows that to reach the same displacement the force necessary are higher for the exterior smooth surface design than for the jagged surface design. This unexpected result will be further commented lather in this section.

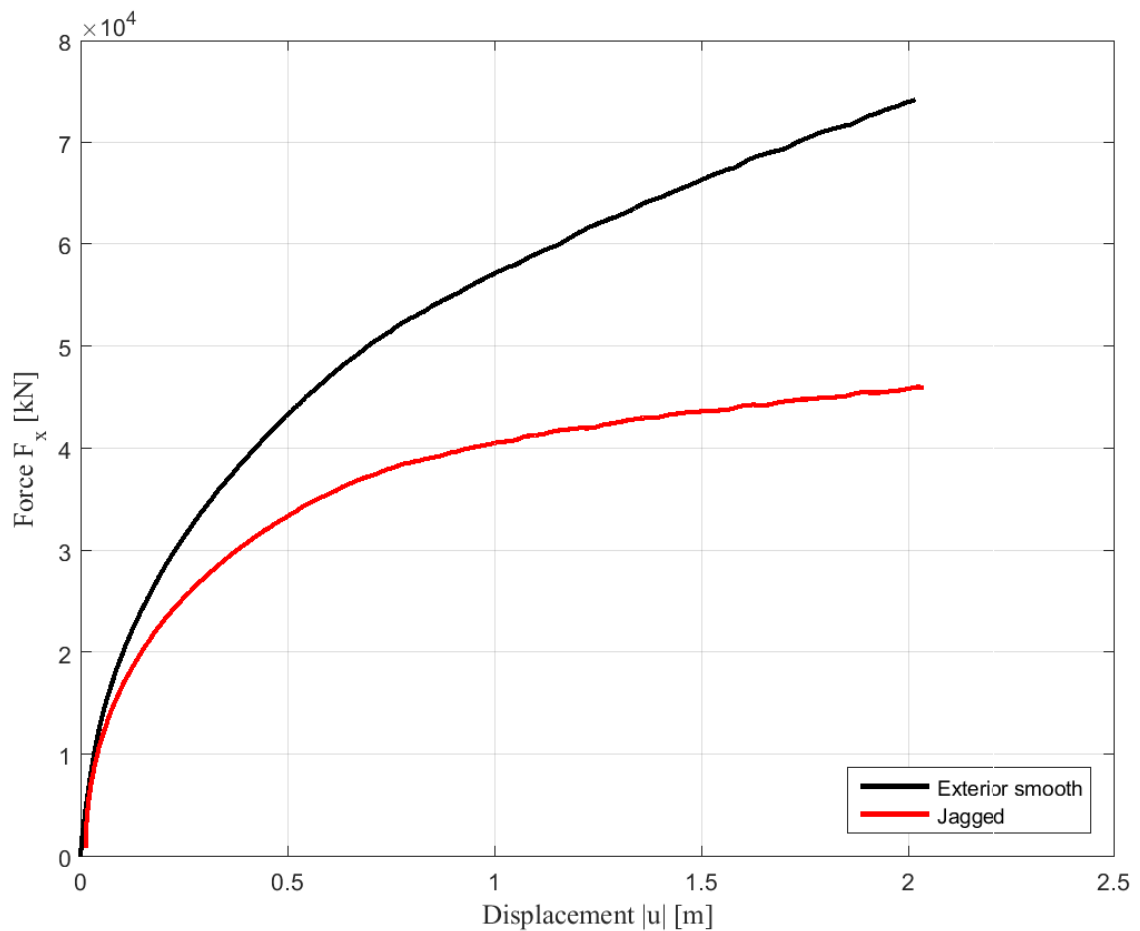


Figure 2.20. Load-displacement curves whit a forced displacement on 2.0 m.

Figure 2.20 is showing the same patten as Figure 2.19. Again the forces necessary to create the prescribed displacement are higher for the exterior smooth surface design than for the jagged surface design. This patten indicates that the supposed surface design is not a good proposal when it comes to the soil-structure relationship.

Because of the unexpected development the axial displacement is also examined. The reason for examining the axial displacement is to check if it is the model which is making an error or if changing to the supposed surface design wont give a reduction of the material cost.

To examine the axial displacement a prescribed displacement will be added to each of the models and again the load-displacement curves will be compared. Figure 2.21 shows where the prescribed displacement is added.

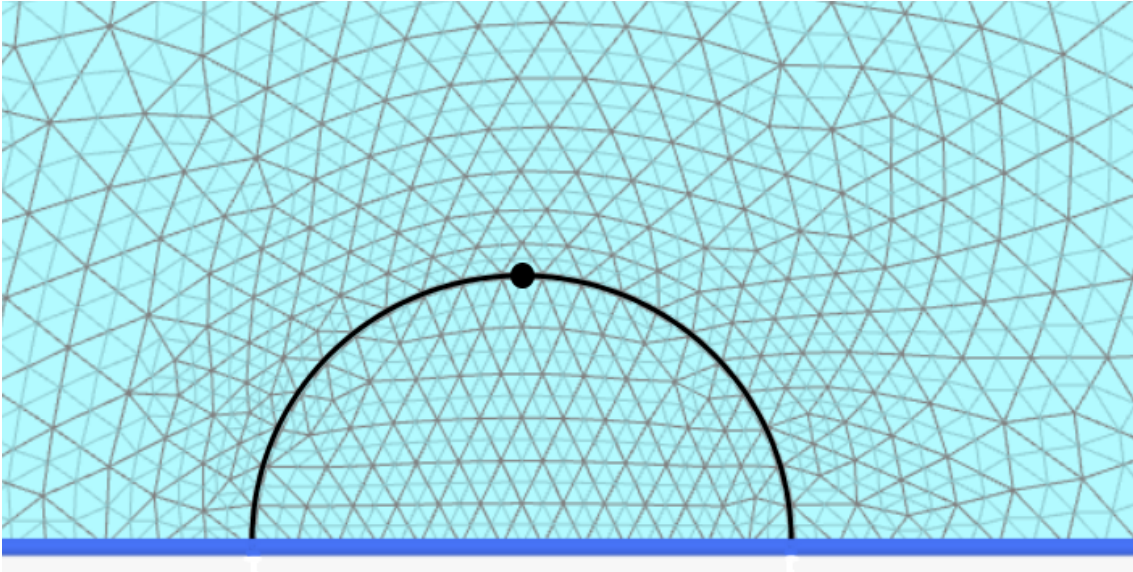


Figure 2.21. Placement of the prescribed displacement.

From a prescribed displacement located as shown in Figure 2.21 valued to 0.50 m is the deformed mesh shown in Figure 2.22 and the curves in Figure 2.23 determined.

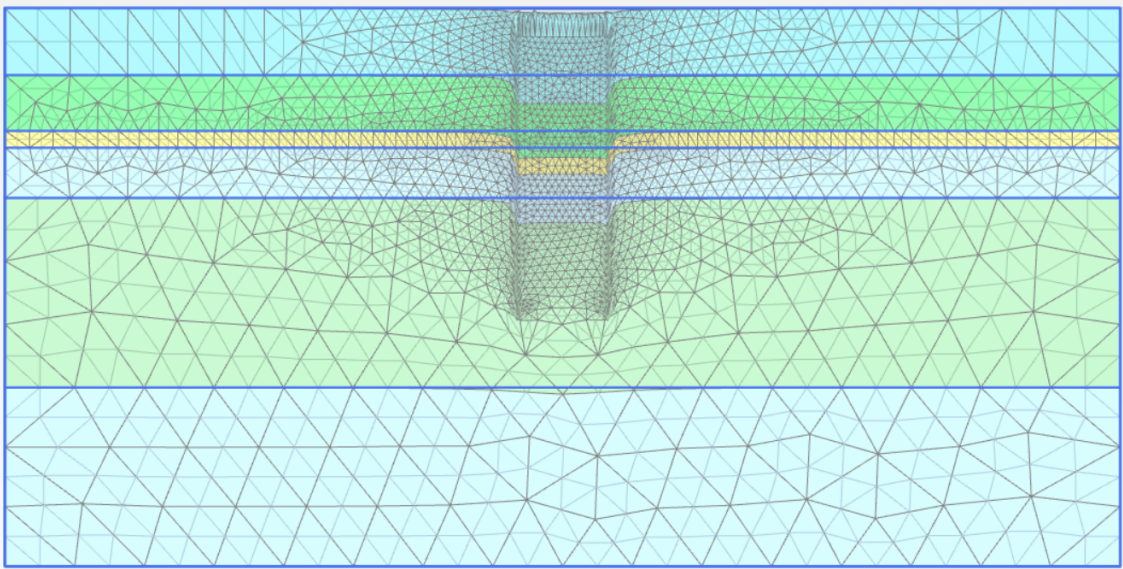


Figure 2.22. Deformed mesh.

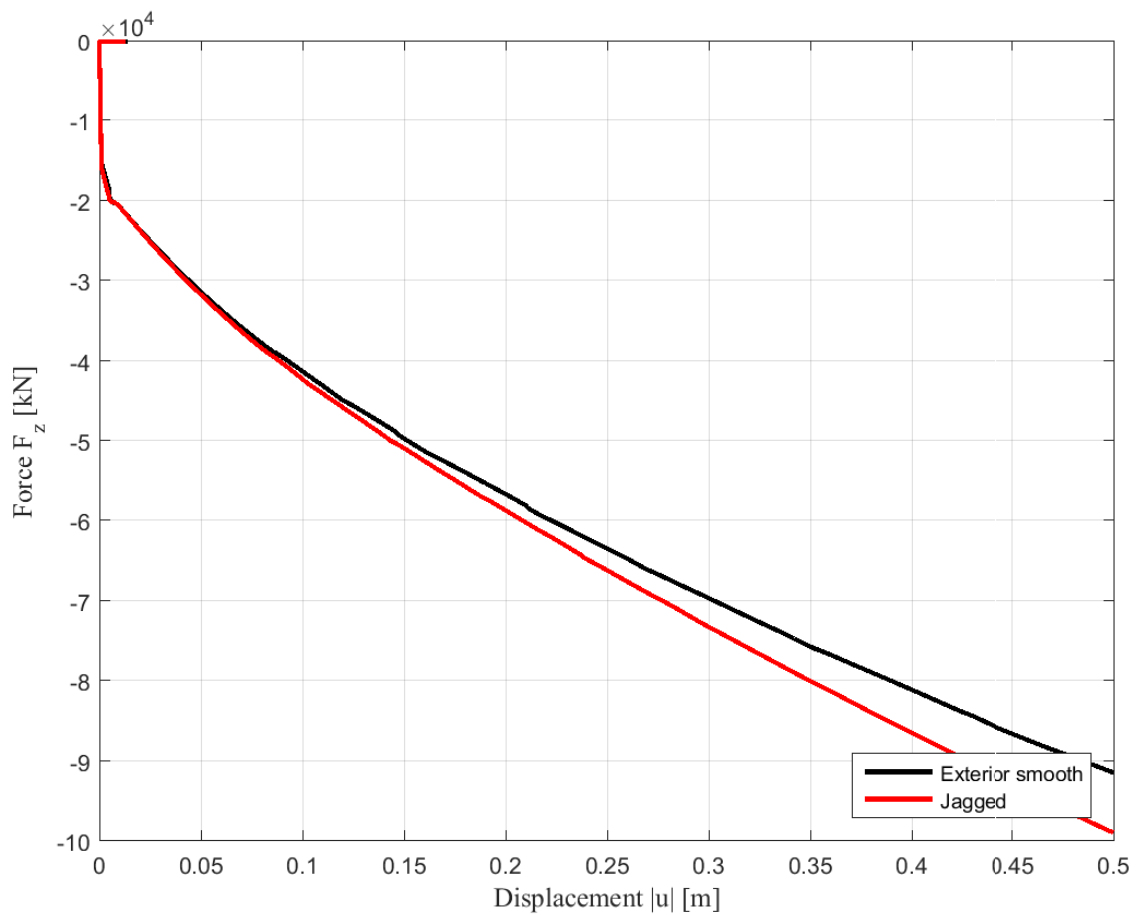


Figure 2.23. Load-displacement curves for axial loaded piles.

From Figure 2.23 it's seen that the forces necessary to force the displacement is numerically higher for jagged surface design. This was more like the result that was expected. This can indicate that an error is made by the PLAXIS program when determining the load-displacement curve for the exterior smooth design with an laterally loaded pile.

1D pile model 3

In this chapter the theory for the methods to describe the load-displacement relationships used in this projekt will be presented. The relationships used in this project are $t(z)$, $Q(z)$, and $p(y)$. The relationships is described according to DNV GL AS [2016] if there is not noted otherwise.

To simplify the 3D model a 1D model will be established and the theory used for the 1D model will be described in the following.

Pile foundations should be designed to withstand static and cyclic loads. Environmental developed loading conditions such as storm waves is cyclic loading, this includes inertial loading. Cyclic loading can potentially have two counteractive effects on the static capacity, repetitive loadings may cause temporary or permanent decrease in the load carrying capacity, and/or accumulate deformations [American Petroleum Institute, 2005].

To determine the soil-structure interaction the Winkler model is used as described in the following section.

3.1 Winkler model

This section is based on [Aron Caselunghe, 2012].

The Winkler model is the simplest method to describe the subgrade, consisting of an infinite number of springs on a rigid base. A sketch of a structural model with infinite number of springs on a rigid base is shown in Figure 3.1.

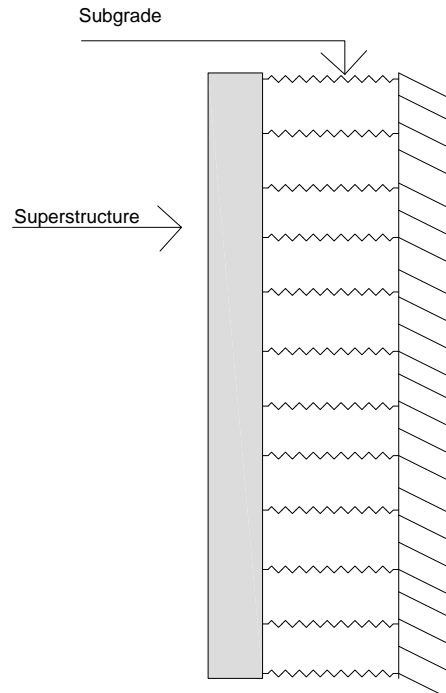


Figure 3.1. Sketch of Winkler model [Aron Caselunghe, 2012].

The Winkler model is implemented easily in a structural system. In a 2D structure the element, is attached to a linespring, similar to a line load but with springs instead, which is attached in the subgrade. The affect of the springs on the structure are only in the horizontal direction. Each spring are attached to two nodes, the nodes on the right side can be removed from the equations because they are fixed, this means that nodes "outside" the superstructure aren't added to the system of equations.

For a discrete spring, k_i the stiffness can be estimated from different approaches, but it is always defined by the relation between the reaction force R_i and the settlement δ_i in one point. The stiffness in one specific point can be written as

$$k_i = \frac{dR_i}{d\delta_i} \quad (3.1)$$

The simplest structural model is the Winkler model, but it is also the least accurate. The model neglect the shear capacity of the soil, which is its primary deficiency. As a consequence of omitting the shear stresses, the displacement has no transverse spread. Therefore, there are discontinuities appearing in the displacement between the loaded and unloaded surfaces. This discontinuities will not occur in reality because soil has a shear capacity. These discontinuities are illustrated in Figure 3.2 and 3.3. The lack of the shear transfer is having an immediate consequence concerning the stiffness at the foundation of the superstructure's edges.

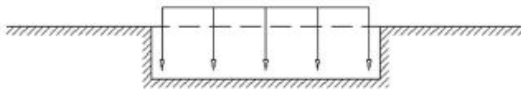


Figure 3.2. Modelled vertical displacement according to the Winkler model [Aron Caselunghe, 2012].

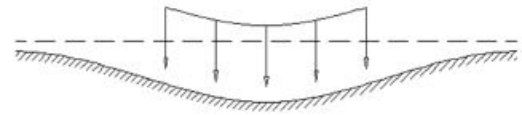


Figure 3.3. Often observed vertical displacement in reality [Aron Caselunghe, 2012].

This lack of the shear transfer can have an effect on how the soil-structure interaction in the area where the different sections of the monopile changes and where the soil layers are changing. The effect could be as shown in the figures above, when a section change the vertical displacement from the different sections does not effect each other, the same would be the case when the soil layers are changing.

In this project the Winkler model could effect in how the surface changes are modelled in the model for the jagged surface design. The Winkler model wouldn't have an effect on the exterior smooth surface design, because there isn't any change on the surface.

3.2 Statical systems

Using the Winkler model the following statical systems for the 1D models are determined. For the axial loaded pile the statical system is shown in Figure 3.4, while the statical system for the laterally loaded pile is shown in Figure 3.5

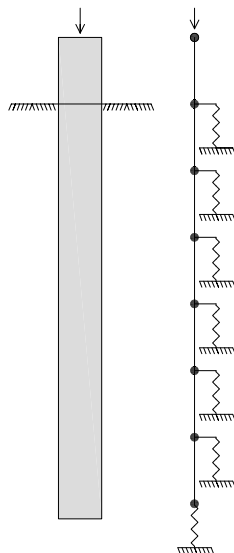


Figure 3.4. Statical system for axial loaded pile.

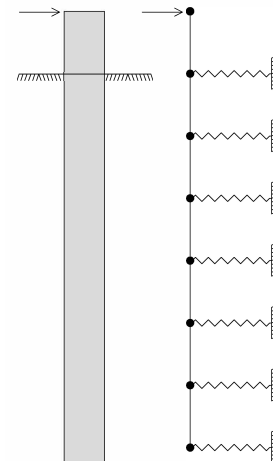


Figure 3.5. Statical system for laterally loaded pile.

To determine the bearing capacity of the monopile the pile stiffness is an important factor. The pile stiffness is making sure that the piles displacements do not reach an unsatisfying level under the loads acting on the monopile during the time it is supporting the wind turbine.

3.3 Load-displacement relationships

During determination of the load capacity of a pile the relative deformations between the soil and the pile should be taken into consideration as well as the compressibility of the soil-pile system. Equation (3.2) shown below assumes that the maximum end bearing capacity of the pile tip and the maximum skin friction along the pile are mobilized simultaneously. However, the ultimate end bearing is not necessarily directly additive to the ultimate skin friction, nor are the ultimate skin friction increments along the pile necessarily directly additive. This effect may, in some circumstances, result in the load carrying capacity being less than that given by equation (3.2) [American Petroleum Institute, 2005].

3.3.1 Axial resistance

To determine the axial pile resistance, R , in a stratified soil deposit of N soil layers equation (3.2) is used. The pile resistance is composed of two parts, one part is the accumulated skin resistance, R_S , and the other part is the tip resistance, R_T .

$$R = R_S + R_T = \sum_{i=1}^N f_{S_i} A_{S_i} + q_t A_t \quad (3.2)$$

where

f_{S_i}	Average skin friction along the pile shaft in layer i
A_{S_i}	Area of the pile shaft in layer i
q_t	Unit resistance
A_t	Gross area of the pile tip

How to determine the non area parameters, skin friction and unit resistance, depends on the soil type and this will be described in the following.

The relationship between the local pile deflection and the mobilized soil-pile shear transfer at any depth is described by using t - z curves in which t is the skin friction and z is the displacement. Likewise, the relationship between the mobilized end-bearing capacity and the axial point bending is described by Q - z curves [American Petroleum Institute, 2005], in which Q is the mobilized end bearing capacity and z is again the displacement.

The t - z curves depends on whether the soil is sand or clay. The parameters used for the t - z curves are the diameter of the pile, the initial shear modulus of the soil, the skin friction resistance and the maximum skin friction resistance. An example of a t - z curves is shown in Figure 3.6.

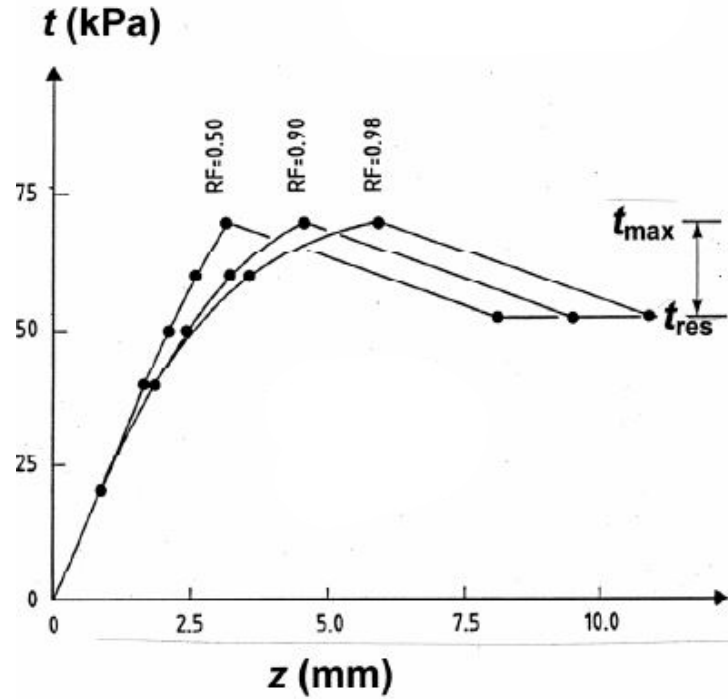


Figure 3.6. Example of t - z curves. [DNV GL AS, 2016]

T-z curves

The t - z curves are used to describe a nonlinear relation between the origin of the skin friction resistance and the point where the maximum skin friction resistance t_{max} is reached. The t - z curve are described in equation (3.3).

$$z = t \frac{R}{G_0} \ln \frac{z_{IF} - r_f \frac{t}{t_{max}}}{1 - r_f \frac{t}{t_{max}}} \quad \text{for } 0 \leq t \leq t_{max} \quad (3.3)$$

where

R	External radius of the pile
G_0	Initial shear modulus of the soil
z_{IF}	Radius of the zone of influence around the pile divided by R
r_f	Curve fitting factor

When the displacement, z , is beyond where the t_{max} is reached the skin friction t decreases until a residual skin friction, t_{res} , is reached, the decrease is linear. When t_{res} is reached and there still occurs displacements the skin resistance becomes constant.

Q-z curves

The tip bearing capacity is determined as equation (3.8) for clay and (3.10) for sand. To mobilize the full tip bearing capacity relatively large tip movements of the pile is required. For full mobilization of the tip bearing capacity in soil may require displacement up to 10

% of the pile diameter. The recommended curves for sand and clay is shown in Figure 3.7 [American Petroleum Institute, 2005].

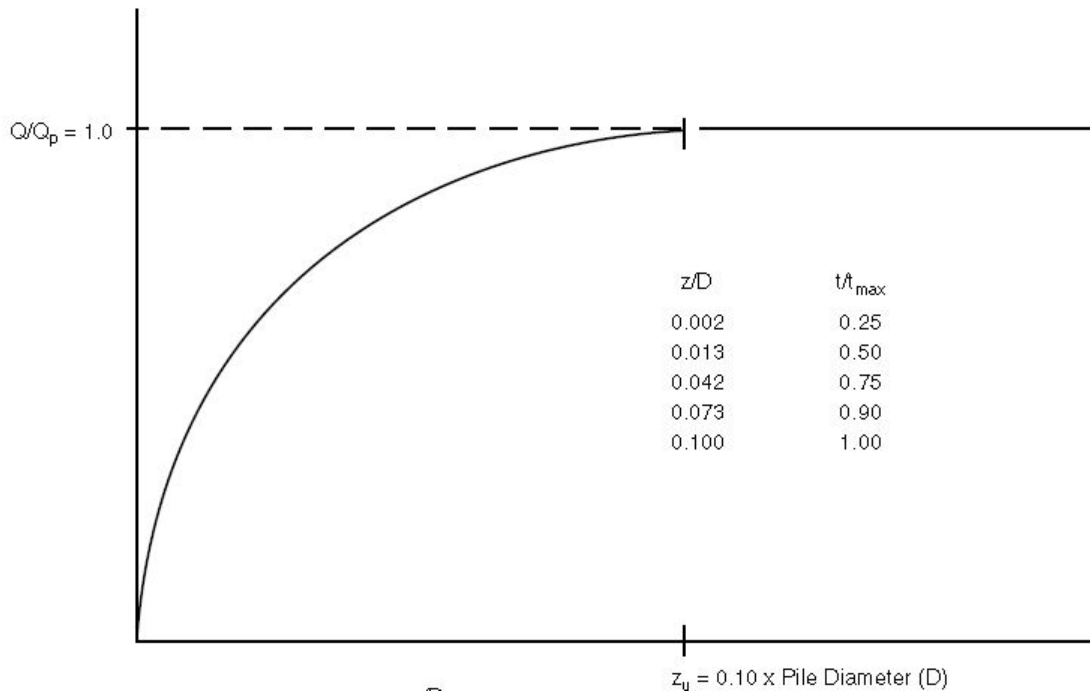


Figure 3.7. Example of Q - z curves. [American Petroleum Institute, 2005]

In which

$\frac{z}{D}$	$\frac{Q}{Q_p}$
0.002	0.25
0.013	0.50
0.042	0.75
0.073	0.90
0.100	1.00

where

z	Axial tip deflection
D	External pile diameter
Q	Mobilized end bearing capacity
Q_p	Total end bearing capacity determine from equation (3.8) or (3.10)

In the following the methods to determine the parameters for equation (3.2) will be described for clay and sand respectively.

Clay

For mainly cohesive soils the average skin friction can be determined from one of the following methods.

Total stress method

This could be the α method where

$$f_{S_i} = \alpha s_u \quad (3.4)$$

with

$$\alpha = \begin{cases} \frac{1}{2\sqrt{s_u/p'_0}} & \text{for } \frac{s_u}{p'_0} \leq 1.0 \\ \frac{1}{2^4\sqrt{s_u/p'_0}} & \text{for } \frac{s_u}{p'_0} > 1.0 \end{cases} \quad (3.5)$$

where

s_u	Undrained shear strength for the soil
p'_0	Effective overburden pressure

Effective stress method

This could be the β method where

$$f_{S_i} = \beta p'_0 \quad (3.6)$$

The β valued is suggested in the range 0.10 to 0.25 for pile length exceeding 15 m

Semi-empirical λ method

This method take all the soil deposits into one layer and then the skin friction is calculated.

$$f_S = \lambda (p'_{0m} + 2s_{um}) \quad (3.7)$$

where

λ	Dimensionless coefficient, depending on pile length as shown in Figure F-1 in DNV GL AS [2016]
s_{um}	Average undrained shear strength along the pile haft
p'_{0m}	Average effective overburden pressure between the pile head and the tip

The tip resistance is determine by

$$q_p = N_c s_u \quad (3.8)$$

where

N_c	= 9 [DNV GL AS, 2016]
s_u	Undrained shear strength at the tip of the pile

Sand

For the friction soils the average skin friction can be determined as

$$f_S = K p'_0 \tan \delta \leq f_1 \quad (3.9)$$

where

K	= 0.8 for open-ended and 1.0 for closed-ended piles [DNV GL AS, 2016]
p'_0	Effective overburden pressure
δ	Angel of soil friction on the pile wall given in Table F-1 in DNV GL AS [2016]
f_1	Limited unit skin friction given in Table F-1 in DNV GL AS [2016]

The tip resistance in friction soils is determined from

$$q_p = N_q p'_0 \leq q_1 \quad (3.10)$$

where

N_q	Bearing factor, can be taken from Table F-1 in DNV GL AS [2016]
q_1	Limited tip resistance given in Table F-1 in DNV GL AS [2016]

3.3.2 Laterally loaded piles

In this section will $y = u_x$.

The most commonly used method to analyse laterally loaded piles is by using the so-called p - y curves. P - y curve gives the relationship between the integral value p of the mobilized soil resistance when the pile deflects a distance y laterally. To model the pile a number of consecutive beam-column elements is used, where nonlinear springs are supporting the element this is also illustrated in Figure 3.1. The p - y curve characterize the nonlinear support spring, an example of the p - y is shown in Figure 3.8 [American Petroleum Institute, 2005].

For a lateral pile deflection y , p is called the lateral resistance per unit length.

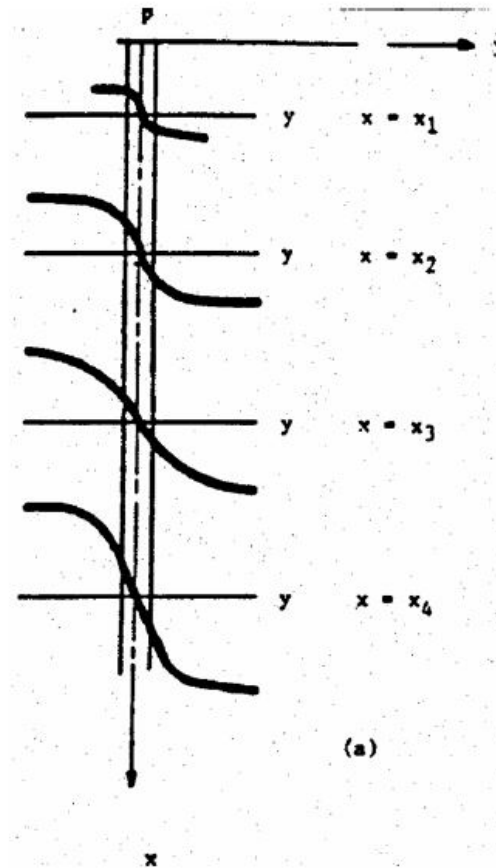


Figure 3.8. Example of P - y curves. [DNV GL AS, 2016]

The pile displacement and stresses in any point along the pile for the applied load at the pile head results as the solution to the differential equation of the pile

$$EI \frac{d^4 y}{dz^4} - p(y) = 0 \quad EI \frac{d^4 y}{dz^4} + q = 0 \quad (3.11)$$

with

$$EI \frac{d^3 y}{dz^3} = Q_L \quad (3.12)$$

$$EI \frac{d^2 y}{dz^2} = M \quad (3.13)$$

where

z	Denotes the position along the pile axis
y	Lateral displacement of the pile
EI	Flexural rigidity of the pile
Q_L	Shear force in the pile
$p(y)$	Lateral soil reaction
q	Distributed load along the pile above soil surface
M	Bending moment in the pile

To construct the p - y curves, the type of loading, the soil type, the remoulding of the soil due to pile installation and the scour effect should be considered. A recommended method to construct the p - y curves is presented in the following.

How to determine the lateral resistance is described in the following. p_u denotes the static ultimate lateral resistance per unit length and is the maximum value p can have when the pile deflect laterally.

Clay

The ultimate lateral resistance for piles in cohesive soil is recommended to be determined as

$$p_u = \begin{cases} (3s_u + \gamma'Z)D + Js_uZ & \text{for } 0 < Z \leq Z_R \\ 9s_uD & \text{for } Z > Z_R \end{cases} \quad (3.14)$$

where

Z	Depth below the soil surface
Z_R	Transition depth, below which the value of $(3s_u + \gamma'Z)D + Js_uZ$ exceeds $9s_uD$
D	External pile diameter
s_u	Undrained shear strength of the soil
γ'	Effective unit soil weight
J	Dimensionless empirical constant valued in the range of 0.25 to 0.50

Sand

The static ultimate lateral resistance in cohesionless soil is recommended to be determined as

$$p_u = \begin{cases} (C_1X + C_2D)\gamma'Z & \text{for } 0 < Z \leq Z_R \\ C_3D\gamma'X & \text{for } Z > Z_R \end{cases} \quad (3.15)$$

where

C_i	Coefficients which depends on the friction angle as shown in Figure F-4 DNV GL AS [2016]
Z_R	Transition depth, below which the value of $(C_1X + C_2D)\gamma'X$ exceeds $C_3D\gamma'Z$
γ'	Submerged unit soil weight

A p - y curve is generated as

$$p = Ap_u \tanh\left(\frac{kZ}{Ap_u}y\right) \quad (3.16)$$

where

k	Initial modulus of subgrade reaction and depends on the friction angle as shown in Figure F-5 DNV GL
A	Factor to account for static or cyclic loading

This will be used in the finite element analyse in chapter 4 of the monopile design to describe the displacements of the monopile under load conditions used in this project.

1D Finite Element Model 4

In this chapter the 1D finite element model will be presented and its results will be shown and compared.

In order to investigate if it is possible to make a simpler model than the 3D model which give the same results as the 3D model a 1D FE model is established.

Again there will be made two FE models one for the exterior smooth surface design and one for the jagged surface design. Many of the input parameters are the same in both models and therefore all the input parameters are described in the same section.

4.1 Input parameters

To establish the FE models it's necessary to know the input parameters, therefore the input parameters to be used are presented in the following.

4.1.1 Soil

The soil parameter used in these models are the same as for the 3D model and are presented in Table 1.2, further the parameters presented in Table 4.1 are also used.

Soil layer	Depth [m]	δ [deg]	f_1 [kPa]	N_q [-]	q_1 [MPa]	J	ρ [kg/m ³]
Sand 1	-38.5, -44.5	20	67	12	2.9	-	2088
Sand 2	-44.5, -49.5	20	67	12	2.9	-	2139
Clay 1	-49.5, -51.0	-	-	-	-	0.5	2038
Sand 3	-51.0, -55.5	25	81	20	4.8	-	2139
Sand 4	-55.5, -72.5	20	67	12	2.9	-	2139
Sand 5	-72.5, -88.5	25	81	20	4.8	-	2139

Table 4.1. Soil parameters, the symbols will be explained in the text.

It is assumed that the sand layer 1, 2 and 4 have a loose density, because of the low friction angle while the other sand layers, 3 and 5, is assumed to have a medium density also based on the friction angle.

δ describes the angle of soil friction on the pile wall, the value is assumed from Table F-1 in DNV GL AS [2016] based on the assumption about loose or medium density mentioned above. f_1 describes the limited unit skin friction, its value is given in Table F-1 in DNV GL AS [2016]. N_q is a bearing factor and the value is taken from Table F-1 in DNV GL

AS [2016]. q_1 is a limited tip resistance and its value is assumed from Table F-1 in DNV GL AS [2016]. J is a dimensionless empirical constant which value is recommended to 0.50 [DNV GL AS, 2016].

To determine the density of the soil equation (4.1) is used. In the equation γ_i is the soil unit weight and g is the gravitational constant.

$$\rho_i = \frac{\gamma_i}{g} \quad (4.1)$$

4.1.2 Monopile

The parameters for the monopile are the upper and lower boundary, the diameter of the pile, the wall thickness, Young's modulus and Poisson's ratio. For steel Young's modulus and Poisson's ratio are respectively $E = 0.21 \times 10^9 \text{ kN/m}^2$ and $\nu = 0.3$ [Jensen et al., 2010]. The upper and lower boundary, the diameter of the pile and the wall thickness are given in Table 1.1.

4.1.3 Load

The load for the laterally loaded models are determined from the PLAXIS models and is based on prescribed displacements. The load for the axially loaded models are based on the masses described in section 1.3.3. The load for the specific analyses is described in the following.

Axial

The axial loading is determined from the masses described in section 1.3.3. The masses which have an influence on the loading of the monopile is the wind turbine tower, the transition piece and the weights presented in Table 1.3. The load is determined as

$$P_z = (m_{tower} + m_{TP} + m_{table}) g = 1158 \text{ kN} \quad (4.2)$$

Laterally

The load in for the laterally loaded piles are determined from the prescribed displacement and is calculated by PLAXIS.

To compare the 1D models a horizontal load at the height of the nacelle is used. The magnitude of the load is determined to be 3000 kN for the comparison of the 1D models. The magnitude of the load is chosen so the bearing capacity is found and this is when the soil body breaks.

4.2 Model build up

When the input parameters are inserted the first which has to be determined is what kind of elements the model is using. In these models the elements used are bar elements. For the axially loaded piles, this means that each element has two degrees of freedom. For the laterally loaded piles the pile is modelled by beam elements, which means that the elements have two degrees of freedom in each node. When the element type is determined,

the next is to determine the kind of analyses to be made, whether it is an axial or a lateral loaded pile being analysed.

4.2.1 Stiffness of the pile

When these decision are made the stiffness matrices can be made. How the stiffness matrices are made is described in Appendix D.

4.2.2 Stiffness of the soil

When the stiffness matrix is created, the soil stiffness have to be determined. The soil stiffness is modelled by the Winkler model as described in section 3.1.

4.2.3 Statical systems

When the stiffnesses are determined the statical systems have to be determined. How each statical system is determined depends on the direction the pile is loaded and the stiffness of the soil and the pile. The statical systems are described in section 3.2.

4.2.4 Displacement curves

When the statical systems are described the displacement curves can be generated. The curves generated are t - z , Q - z and p - y curves, how the curves are determine is described in chapter 3.

4.3 Results

The results from the F.E.M. will be presented first for the exterior smooth surface and then the results for the jagged surface. After the results have been presented a comparison between the two surface designs will be made.

4.3.1 Exterior smooth surface

From the axial loaded pile the t - z curves for the exterior smooth surface is shown in Figure 4.1.

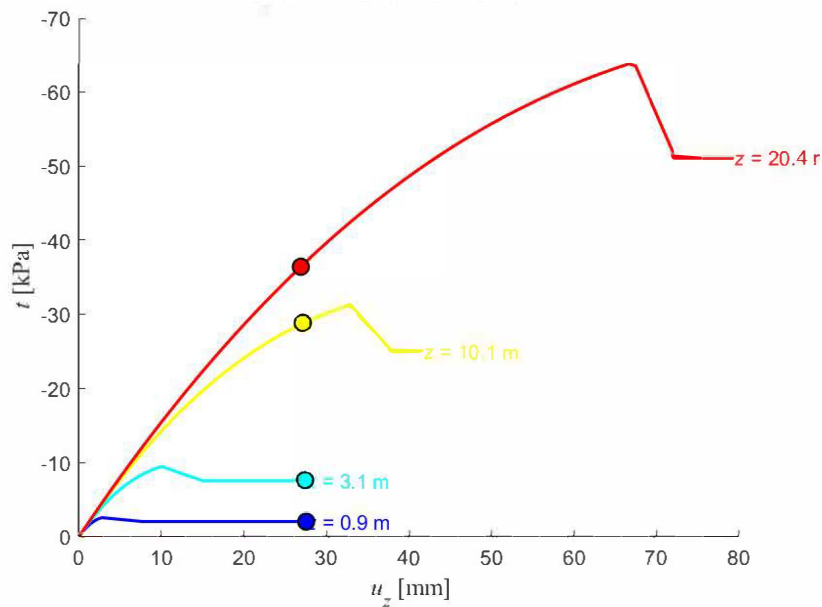


Figure 4.1. t - z for chosen locations.

The placement of the t - z curves can be seen in Figure 4.2. The meters on the z axis is from the soil surface and not from the Mean water level.

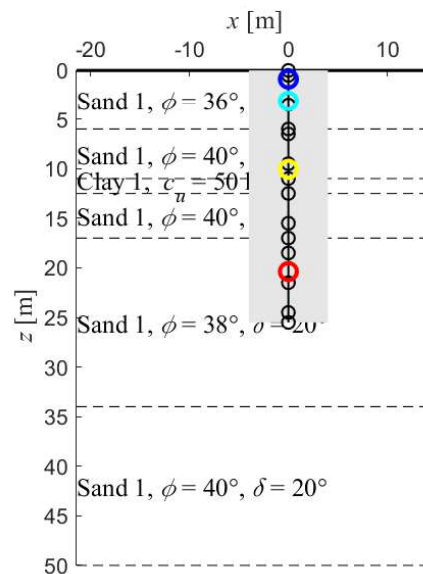


Figure 4.2. Locations for the t - z curves.

It can be seen in Figure 4.1 for the two first locations for the curves, the two blue points located at a depth of respectively 0.9 m and 3.1 m below the soil surface, that the the maximum skin friction resistance t_{max} is reached, at a value of respective -3 kPa and -10 kPa. The skin friction has also reached the residual skin friction t_{res} at these locations at a value of respective -2 kPa and -8 kPa. At the location for the two curves at a lower depth, the yellow and the red, the t - z curves has not reached the maximum skin friction resistance. This means that the skin friction still can help carrying more load than it does.

The Q - z curve is shown in Figure 4.3. It can be seen in the figure that the displacement at the tip is 26.8 mm. It can also be seen from the load displacement relationship that the initial bearing capacity is not reached, if the initial bearing capacity had been reached the red dot at the curve would have been placed where the curve is parallel to the u_{tip} axis.

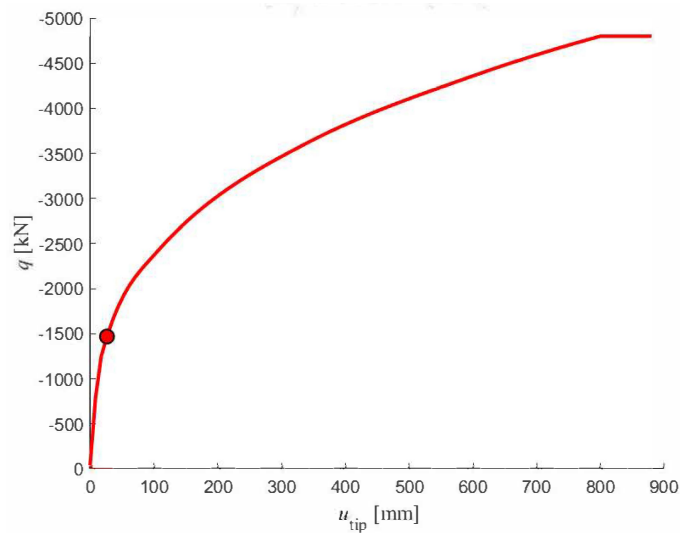


Figure 4.3. Q - z curve for the exterior smooth surface.

From the laterally loaded pile the displacement curves and the p - y of the exterior smooth surface shown is in Figure 4.4 and 4.5. It can be seen in Figure 4.4 that the displacement for the monopile is 0.34 m at the top of the pile.

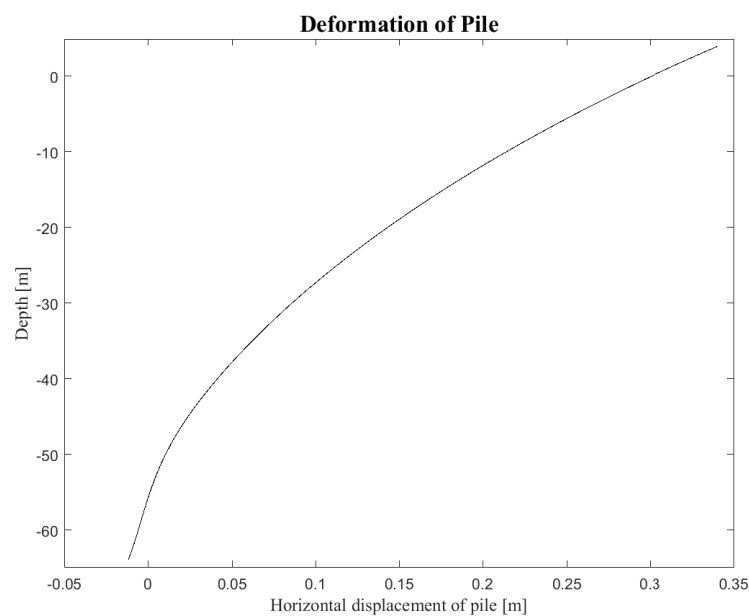


Figure 4.4. Displacement curve for the exterior smooth surface.

The p - y curves indicate that the soil body is failed at depth -38.75 m and at depth -41.4 m, this indication is shown as the red star is located where the curves has reached a phase where the deformation is increasing without the forces is increasing. At the, lower

depths are there no indication of failure of the soil body, this makes sense because the displacement at the lower depths are smaller than at the upper depths.

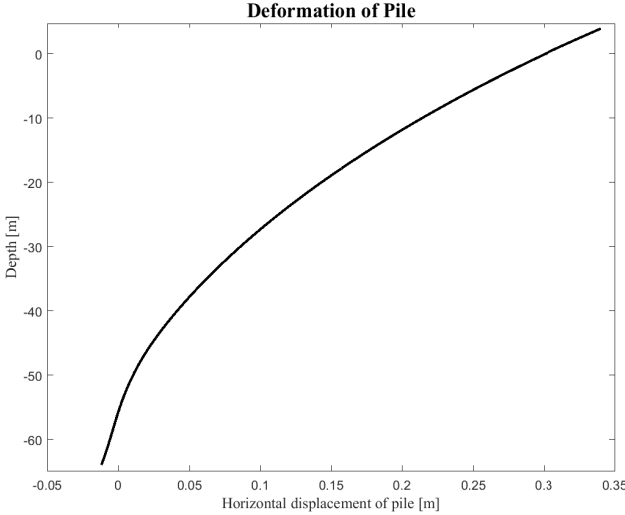


Figure 4.5. *P-y* curve for the exterior smooth surface.

4.3.2 Jagged surface

From the axial loaded pile Figure 4.6 is showing the *t-z* curves for the jagged surfaced monopile. The locations of the *t-z* curves are the same as for the exterior smooth surface design, the location can be seen in Figure 4.2.

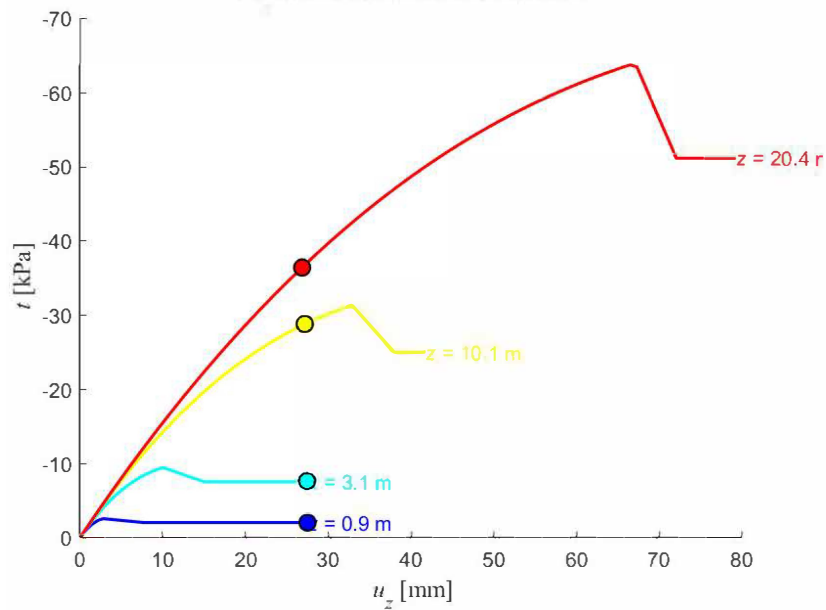


Figure 4.6. t - z for chosen locations.

It can be seen in Figure 4.6 that the maximum skin friction resistance t_{max} is reached for the two first locations for the curves, the two blue points located at a depth respectively 0.9 m and 3.1 m below the soil surface. The value for t_{max} are respective -3 kPa and -10 kPa. The skin friction at these locations has also reached the residual skin friction t_{res} valued at respective -2 kPa and -8 kPa. The yellow and red t - z curve shows that the maximum skin friction resistance are not reached at the location of the points. This indicate than the skin friction still can carry more load that it does under the load case.

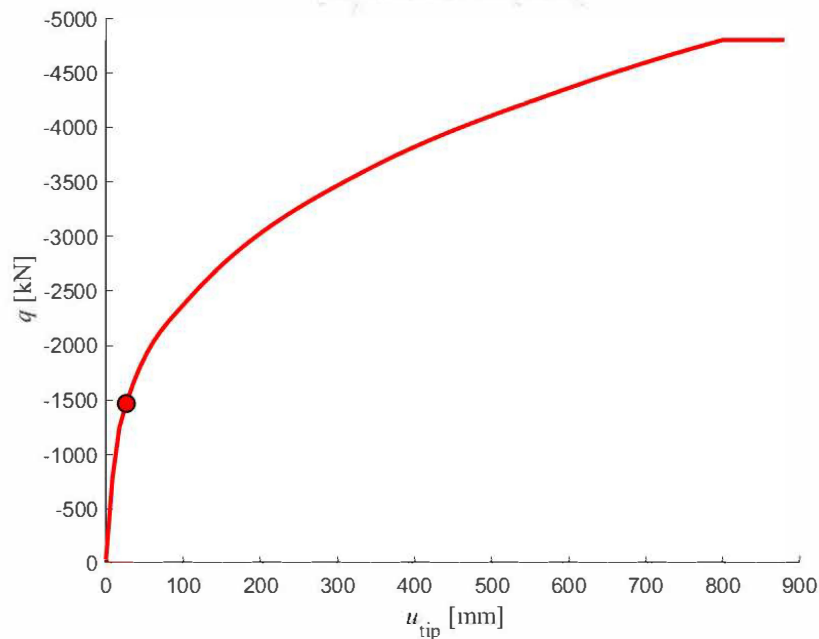


Figure 4.7. Q - z curve for the exterior smooth surface.

The Q - z curve in Figure 4.7 shows that the displacement at the tip is 26.8 mm, which is the same value as for the exterior smooth surfaced monopile. It can also be seen from the load displacement relationship that the initial bearing capacity is not reached for the same reason as for the exterior smooth surfaced monopile.

From the laterally loaded pile the displacement and the p - y curves for the jagged surface design is shown in Figure 4.8 and 4.9.

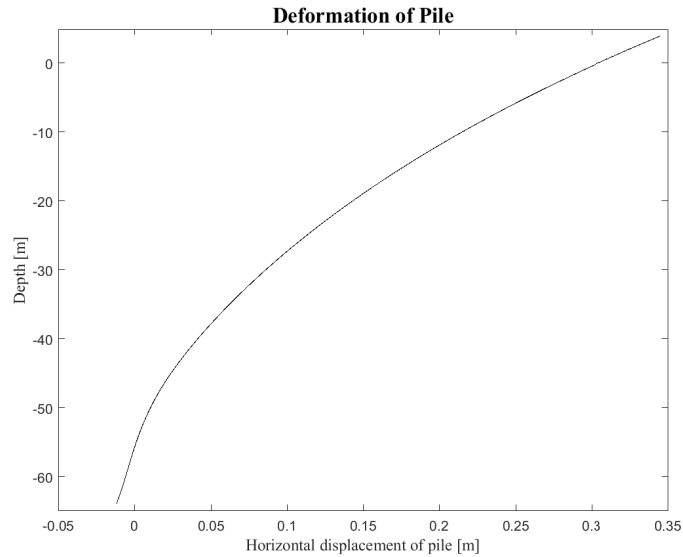


Figure 4.8. Displacement for the jagged surface.

From Figure 4.8 can it be seen that the displacement for the monopile is 0.35 m at the top of the pile. The p - y curves in Figure 4.9 indicate that the soil body at the upper depths, -38.75 m and -41.4 m, is at failure. Again is the indication shown as the red star is located at the curves when the curves are flat. The lower depth curves, -48.42 m and -58.1 m, are indicating that the bearing capacity of the soil isn't reached.

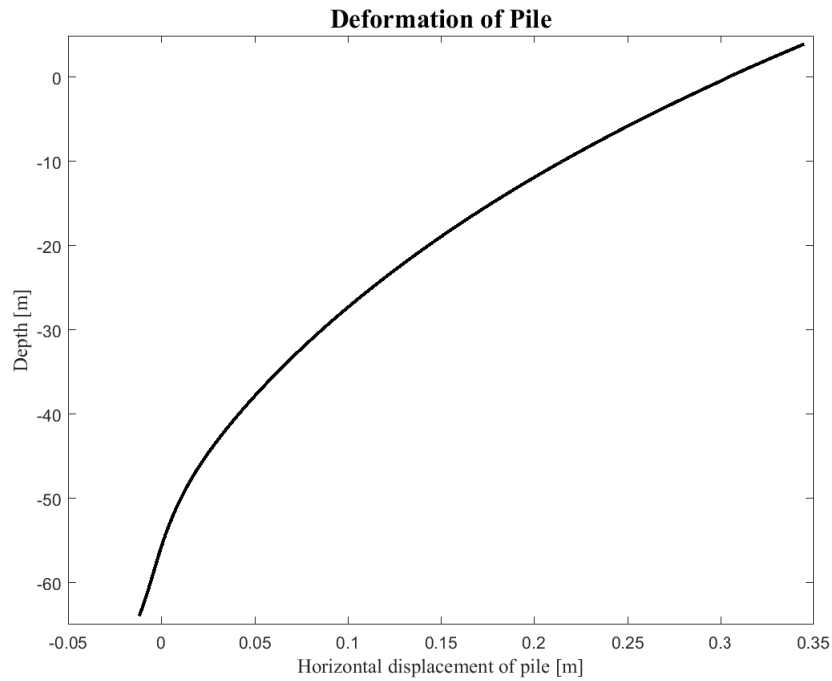


Figure 4.9. P - y curve for the exterior smooth surface.

4.4 Comparison

When comparing the result for the axial loaded piles there are no difference both when the t - z and Q - z curves are compared. If the curves for the different surface designs are plotted in the same graph there is no visible difference, therefore there is no plot shown of the comparison for the axial loaded piles.

For the laterally loaded pile is the displacement and the p - y curves doesn't show large differences between the surface designs but for the p - y curves there is a small difference shown in Figure 4.10. In the figure it is seen that the jagged surface design, the red curve, is slightly higher than the exterior smooth surface design.

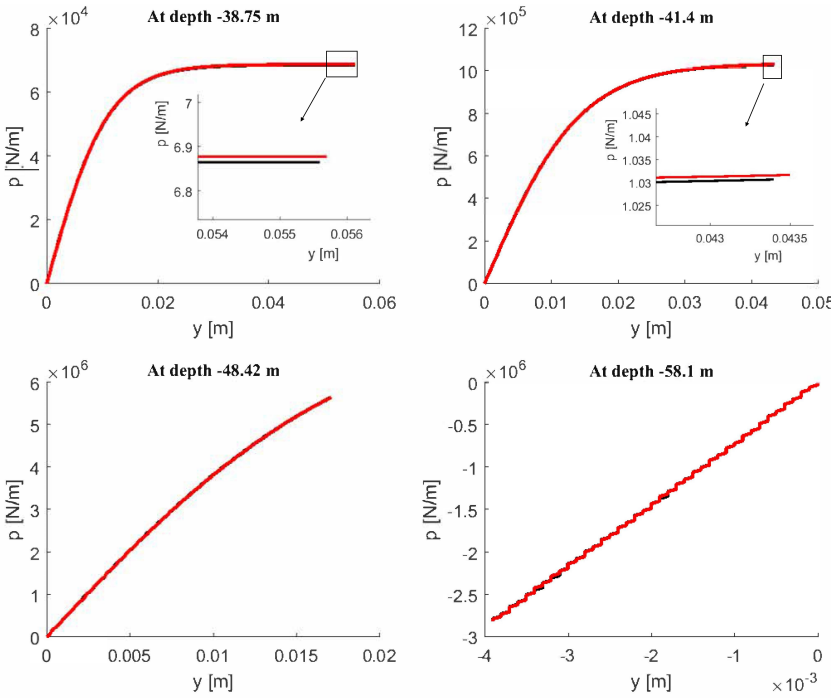


Figure 4.10. P - y curve for the exterior smooth surface.

Based on this comparison is there a possibility that the jagged surface may lead to a small reduction of the material cost.

Conclusion 5

In this chapter a comparison between the 3D models and the 1D models will be conducted. From this comparison a final conclusion will be drawn. After the conclusion a discussion will be made where the results will be discussed and suggestions to further investigations will be given.

5.1 Comparison of calculation methods

To compare the 3D models with the 1D model the displacements from the axial and laterally loaded pile will be compared. The displacement for the models are shown in Table 5.1.

Load	Exterior Smooth		Jagged	
	3D	1D	3D	1D
Axial	0.015 m	0.027 m	0.013 m	0.027 m
Laterally	2.02 m	0.21 m	2.04 m	0.19 m

Table 5.1. Section parameters

Table 5.1 shows that for the axial loaded piles the difference of the displacements between the 3D models and the 1D models are almost the double. A difference was expected between the 3D models and the 1D because the pile in the 3D models is modelled as a rigid body while in the 1D models the pile is modelled as a linear elastic steel pile. Table 5.1 also shows that for the laterally loaded piles there is a factor 10 difference between the 3D models and the 1D models, what this error is cost by is not known at this particular time. It could be that the material parameters used in the 1D models are valued wrong or that there is an error in how the displacements are determined in the 1D models.

When the models are compared it can be concluded that the models don't give the same results but they gives an indication of the possibility of reducing the material cost. Due to the fact that there is a pattern between the surface designs showing that the jagged surface has a smaller displacement than the exterior smooth surface.

When the models have been compared it can also be concluded that there is a possibility of reducing the material cost when the surface design is changed.

5.2 Discussion

In this discussion it will be discussed why the results show that there is a possibility of saving any material while changing the surface design.

5.2.1 Focus

Since the displacements are almost identical there is a possibility of saving material. In the performed calculations the main focus has been on the soil-structure behaviour of the system, but if the focus was on the structure itself the result maybe would have been different. This is because the exterior smooth surface has eccentricities and this courses that the forces have to be transferred to the next element by torque while for the jagged surface design a normal force can transfer the forces instead. This can lead to a reduction of the shear stresses in the elements for the jagged surface design and by this reduction a possible reduction of the material needed for the monopile to retain the bearing capacity of the system.

5.2.2 Loading type

The 1D models set up in this report are built for cyclic loading but so far only results for static loading are shown for the two structure types. The cyclic loading will have an influence on the bearing capacity of the monopile, and this influence will affect both surface designs. However, the effect of the cyclic loading is not examined in this project, but it could lead to some material savings when changing the surface design, due to how the load is transferred as described earlier.

5.2.3 Soil parameters

In this project the initial shear modulus the only modulus used. The initial shear modulus is assumed in the 3D models as the shear modulus this give a reduction of the stiffness of the soil and this leads to larger displacement than those determined in chapter 2.

Bibliography

- 4Coffshore, 2013.** 4Coffshore. *Monopiles Support Structures*.
<https://www.4coffshore.com/windfarms/monopiles-support-structures-aid4.html>, 2013.
Downloaded: 19-09-2018.
- American Petroleum Institute, 2005.** American Petroleum Institute. *Recommended Practice for Planning, Designing and Constructing Fixed Offshore Platforms—Working Stress Design*. 2005.
- Aron Caselunghe, 2012.** Jonas Eriksson Aron Caselunghe. *Structural Element Approaches for Soil-Structure Interaction*, 2012.
- Cook et al., 2002.** Robert D. Cook, David S. Malkus, Michael E. Plesha and Robert J. Witt. *Concepts and applications of finite element analysis*. ISBN: 978-0-471-35605-9. John Wiley and Sons Inc., 2002.
- DNV GL AS, 2016.** DNV GL AS. *Support structures for wind turbines*. 2016.
- Haque, 2016.** Aamer Haque. *Introduction to Timoshenko Beam Theory*.
<http://www.clearlyimpossible.com/ahaque/timoshenko.pdf>, 2016. Downloaded: 20-09-2016.
- Jensen et al., 2010.** Bjarne Chr. Jensen, Gunnar Mohr, Erik Brandt, Bo Mortensen, Lars Pilegaard Hansen, Carsten Munk Plum, Eilif Svensson, Svend Ole Hansen, Finn Olaf Precht Sørensen, Dirch H. Bager, Henning Laustsen, Ejnar Søndergaard, Martin Uhre Mandrup, Jørgen Munch-Andersen, Thomas Cornelius, Lars Zenke Hansen, Per Goltermann, Jørgen S. Steinfeld, Carsten S Sørensen and Egil Borchersen. *Teknisk Ståbi*. Nyt Teknisk Forlag, 2010. ISBN 978-0-7277-4086-1.
- Krabbendam, 4 January 2017.** Richard Krabbendam. *Roermond, the Netherlands*.
<http://www.heavyliftnews.com/news/sif-awarded-the-production-of-all-monopiles-offshore-high-voltage-station-ohvs-pile-and-transition-pieces-for-the-norther-offshore-wind-farm>, 4 January 2017. Downloaded: 19-09-2018.
- PLAXIS, 2018a.** PLAXIS. *PLAXIS 2D Material Models Manual*. 2018.
- PLAXIS, 2017.** PLAXIS. *PLAXIS 3D Reference Manual*. 2017.
- PLAXIS, 2018b.** PLAXIS. *PLAXIS 3D Scientific Manual*. 2018.
- Portali, 2018.** PROKON Support Portali. *Elastic Properties of Soils*.
<https://support.prokon.com/portal/kb/articles/elastic-properties-of-soils>, 2018.
Downloaded: 24-05-2018.
- Vattenfall, 2018.** Vattenfall. *Design Rapport*, 2018.

Monopile A

As mentioned is the design of the monopile determined from Vattenfall and looks as in Figure A.1.

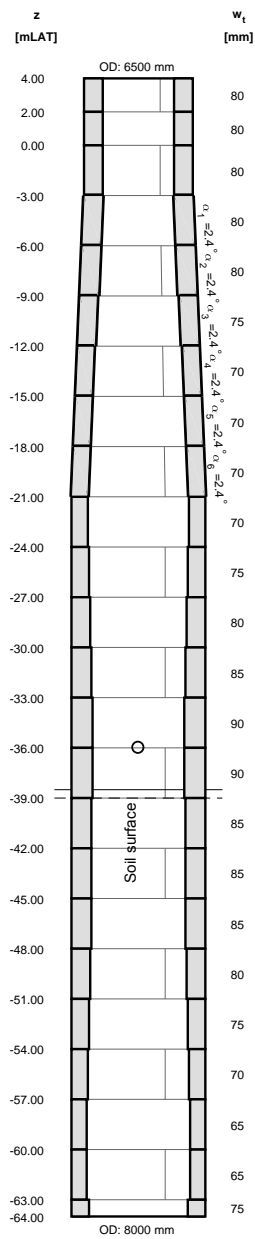


Figure A.1. Monopile Design.[Vattenfall, 2018]

Mohr-Coulomb B

In this chapter the theory for the Mohr-Coulomb model will be described, the description is based on PLAXIS [2018a]. The Mohr-Coulomb model is a well known and simple linear-elastic perfectly plastic model, the model can be used to approximate the soil behaviour. The models linear elastic part is based on Hooke's law, while the perfectly plastic is based on Mohr-Coulomb failure criterion. Development of irreversible strain is involved in plasticity. A yield function is introduced to evaluate if plasticity will occur the yield function is formulated as a function of stress and strains.

In elastoplasticity the strains, ε , and strain rates, $\dot{\varepsilon}$, decomposed into a plastic, ε^p , and an elastic, ε^e , part.

$$\varepsilon = \varepsilon^e + \varepsilon^p \quad \dot{\varepsilon} = \dot{\varepsilon}^e + \dot{\varepsilon}^p$$

Associated plasticity overestimate dilatancy for Mohr-Coulomb type yield functions. Therefore is a plastic potential function introduced in addition to the yield function. The parameters there is used for stress states with in the yield surface is the elastic Young's modulus E and the Poisson's ration ν . The friction angle ϕ and the cohesion c is the plastic parameters in the yield functions. A third plastic parameter is introduced from the plastic potential, this parameter is the dilation angle ψ . Mohr-Coulomb criterion allows tension for $c > 0$, soil can sustain none to very small tensile stresses. In PLAXIS is this behaviour can be included by a tension cut-off, this allows only the used of Mohr circles with negative principal stresses.

The Mohr-Coulomb model takes account for non-associated flow and tension cut-off. The model does not take in account for volume and shear hardening, different responses for primary loading and elastic unloading/reloading and time effect, creep. The model is a simple model because it only uses five parameters, therefore is the model only applied for initial studies.

B.1 Yield condition

The use of six yield functions is needed to formulate the Mohr-Coulomb yield conditions fully, the yield functions are formulated in terms of principal stresses.

A fixed hexagonal cone in principal stress space represents the condition $f_i = 0$ for all the yield functions, the hexagonal cone is shown in Figure B.1

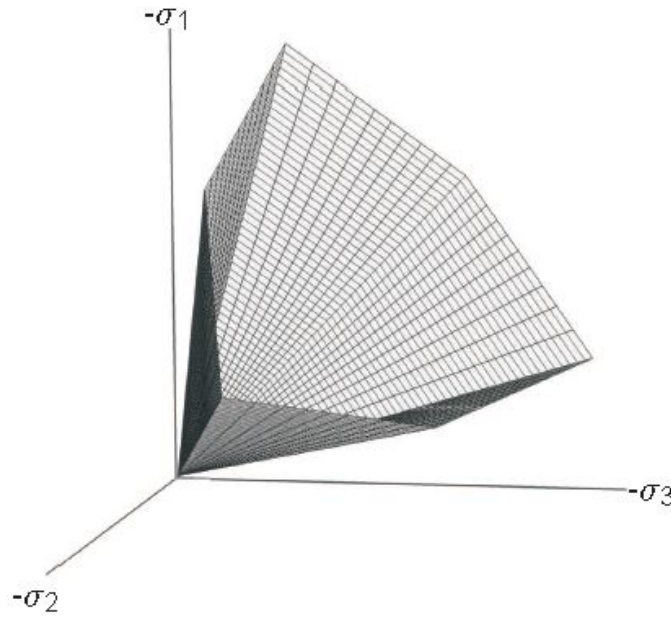


Figure B.1. Hexagonal cone in principal stress space [PLAXIS, 2018a].

Six plastic potential functions are defined in addition to the six yield function.

The Mohr-Coulomb model takes account for non-associated flow and tension cut-off. The model does not take in account for volume and shear hardening, different responses for primary loading and elastic unloading/reloading and time effect, creep. The model is a simple model because it only uses five parameters, therefore is the model only applied for initial studies. Figure B.2 shows the approximation for first order model.

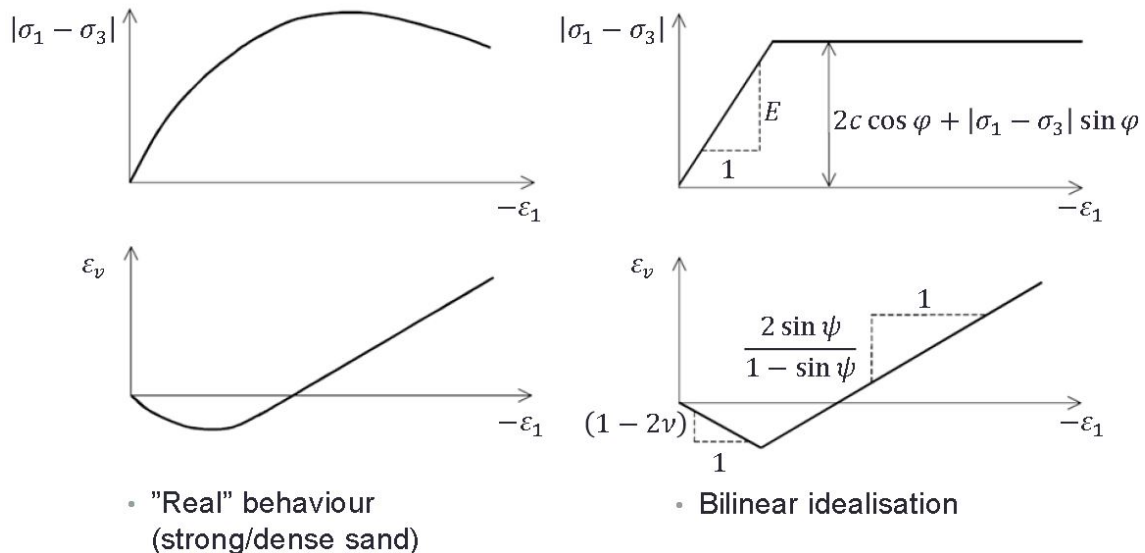


Figure B.2. Principal for Mohr-Coulomb model. [PLAXIS, 2018a].

Elements for 3D model

C

In this chapter the elements used in the 3D models will be described. This chapter is based on [PLAXIS, 2018b]

The soil volume is described with 10 node tetrahedral elements. In the 3D mesh the 10 node tetrahedral elements are created. The interpolation of the displacement is for this type of elements of second order. There are three local coordinates (ξ, η and ζ) for tetrahedral elements. The shape function N_i given at node i have the property that the function is valued to unity and is zero in the other nodes. The shape functions for the 10 nodes are shown in Figure C.1

$$\begin{aligned}
 N_1 &= (1 - \xi - \eta - \zeta)(1 - 2\xi - 2\eta - 2\zeta) \\
 N_2 &= \zeta(2\zeta - 1) \\
 N_3 &= \xi(2\xi - 1) \\
 N_4 &= \eta(2\eta - 1) \\
 N_5 &= 4\zeta(1 - \xi - \eta - \zeta) \\
 N_6 &= 4\xi\zeta \\
 N_7 &= 4\xi(1 - \xi - \eta - \zeta) \\
 N_8 &= 4\eta(1 - \xi - \eta - \zeta) \\
 N_9 &= 4\eta\zeta \\
 N_{10} &= 4\xi\eta
 \end{aligned}$$

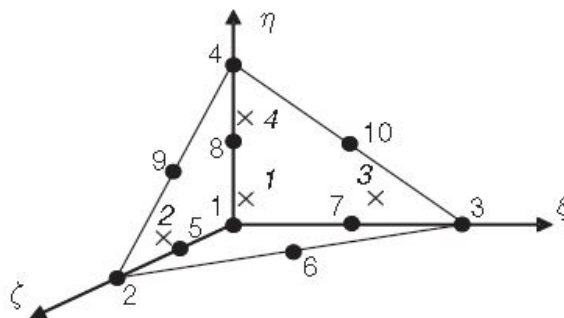


Figure C.1. 10 node tetrahedral element with local numbering and integrations points (x) [PLAXIS, 2018b].

Each node have three degrees of freedom u_x, u_y and u_z .

Finite Element analyses

D

In the chapter the theory used to determine the stiffness matrices will be described.

The beam theory used for the beam in this report is the Timoshenko beam theory. The reason for choosing this theory is that the Euler-Bernoulli beam theory is inaccurate for deep beams. With deep beams the depth cannot be neglected when it is compared to the length. For deep beams a more accurate beam theory or a complete solid mechanics is required. In the Timoshenko beam theory is shear deformations included, where as shear deformations are absent in the Euler-Bernoulli beam theory [Haque, 2016]. For the Timoshenko beam theory the basic assumptions are [Haque, 2016]:

- The unloaded beam is straight in the longitudinal axis.
- Applied loads act transverse to the longitudinal axis.
- Deformations and strains are small.
- Stresses and strains can be relate by Hooke's law.
- Plane cross sections, which are initially normal to the longitudinal axis, will remain plane after deformation.

Only the latter requirement differs from the Euler-Bernoulli theory because Timoshenko for beams plane cross sections will rotate due to shear forces, while Euler-Bernoulli beams states that plane cross sections also remain normal to the beam axis after deformation [Haque, 2016].

The differential equation to described the beam is [Haque, 2016]:

$$EI \frac{d^4 u}{dx^4} = q(x) \quad (D.1)$$

The solution to the differential equation, when using Timoshenko beams and with the dimensionless parameter $\xi = x/L$ and since $q(\xi) = 0$ becomes [Haque, 2016]:

$$P(\xi) = P_0 \quad (D.2)$$

$$M(\xi) = LP_0 \xi + M_0 \quad (D.3)$$

$$\theta(\xi) = \frac{L^2 P_0 \xi^2}{2EI} + \frac{LM_0 \xi}{EI} + \theta_0 \quad (D.4)$$

$$u(\xi) = \frac{L^3 P_0 \xi^3}{6EI} + \frac{L^2 M_0 \xi^2}{2EI} + L \left(\theta_0 - \frac{P_0}{GA_s} \right) \xi + u_0 \quad (D.5)$$

Boundary conditions are used to determine the magnitudes of the constants V_0 , M_0 , θ_0 and u_0 . Also another parameter is needed to be defined. The parameter is Φ , which is essential for formation of the stiffness matrix [Haque, 2016].

D.1 Establishment of stiffness matrix

A finite element analysis have a characteristic matrix for load and deflection analyses called a stiffness matrix. An one-dimensional element characteristic matrix can be formulated by the direct method because they are simple. The direct method is approached by equilibrium considerations.

The number or type of element used does not change the computational procedure for The Finite Element Analyses, F.E.A., which is time independent [Cook et al., 2002].

The procedure for a F.E.A. is as follows [Cook et al., 2002].

1. Generate matrices that describe element behavior [Cook et al., 2002].
2. Connect elements together, which implies assembly of elements matrices to obtain a structure matrix [Cook et al., 2002].
3. Provide some nodes with loads.
4. Provide other nodes with boundary conditions, which may be called support conditions in structural mechanics [Cook et al., 2002].
5. The structure matrix and the array of loads are parts of a system of algebraic equations. Solve these equations to determine the nodal values of field quantities [Cook et al., 2002].
6. Compute gradients: strains in structural mechanics [Cook et al., 2002].

The stiffness matrix is depending of how many degree of freedom, d.o.f., the element have in each node. An element with one d.o.f. is a bar element while an element with two d.o.f. is a beam element a combination of the two elements is called a rod element and have three d.o.f. in each node. Each element type have different stiffness matrices. The stiffness matrix is used to analyse each structural element different structural behaviour under different load conditions.

D.1.1 Bar element

This section is based on [Cook et al., 2002]

A bar element is as mentioned an element which have one d.o.f. in each node. This is illustrated in Figure D.1. As it can be seen in the figure a bar element have two d.o.f. per element. The degree of freedom is denoted in the figure with u_i , the force is denoted F_i for the i 'th node. σA denotes the internal work.

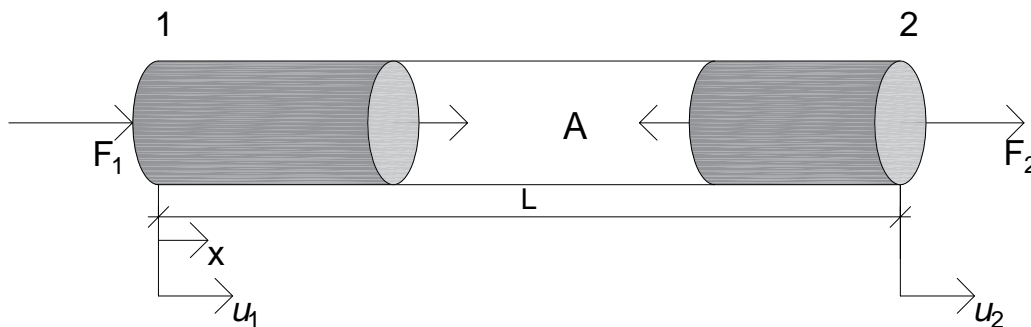


Figure D.1. Sign convention for the bar element

The stiffness of the bar can be approached directly by the equilibrium considerations. The stiffness is determined with use of the kinematic, physical and static conditions. The kinematic condition is the relation between the strains and the displacements, the strains are unidirectional normal because they are constant over the cross section of the bar. The strains are determined as.

$$\varepsilon = \frac{u_2 - u_1}{L}$$

The physical conditions are the stress-strain relationship, which is also known as a constitutive law and for one-dimensional relation can be described by Hooke's law as.

$$\sigma = E\varepsilon$$

The static condition is using equilibrium equations to determine the forces at each node, which is done as follows.

$$\text{At node 1: } F_1 = \sigma A \Rightarrow F_1 + EA \frac{u_2 - u_1}{L} = 0 \Rightarrow \frac{EA}{L}(u_1 - u_2) = F_1$$

$$\text{At node 2: } F_2 = \sigma A \Rightarrow F_2 - EA \frac{u_2 - u_1}{L} = 0 \Rightarrow \frac{EA}{L}(u_2 - u_1) = F_2$$

The equilibrium equations can be expressed as a matrix equation as $[\mathbf{k}]\{\mathbf{u}\} = -\{\mathbf{f}\}$, where $[\mathbf{k}]$ is the stiffness matrix for the bar element, for a two-node bar element with only axial displacements is the matrix a 2×2 matrix. $\{\mathbf{u}\}$ is a vector which contains information about the displacements in the nodes, $\{\mathbf{u}\} = [u_1 \ u_2]^T$. Vector $\{\mathbf{f}\}$ is negative because it is used to mean load associated with deformation, which is applied by an element to structure node. The forces are applied to the element as $-\{\mathbf{f}\} = [F_1 \ F_2]^T$.

This is used as follows

$$\begin{bmatrix} k & -k \\ -k & k \end{bmatrix} \begin{Bmatrix} u_1 \\ u_2 \end{Bmatrix} = \begin{Bmatrix} F_1 \\ F_2 \end{Bmatrix} \quad \text{with} \quad k = \frac{EA}{L}$$

This gives a stiffness matrix for the bar element as

$$[\mathbf{k}] = \begin{bmatrix} \frac{EA}{L} & -\frac{EA}{L} \\ -\frac{EA}{L} & \frac{EA}{L} \end{bmatrix} \quad (\text{D.6})$$

D.1.2 Beam element

This section is based on [Haque, 2016].

A beam element has two d.o.f. in each node, this is lateral translation and rotation. This is shown in Figure D.2

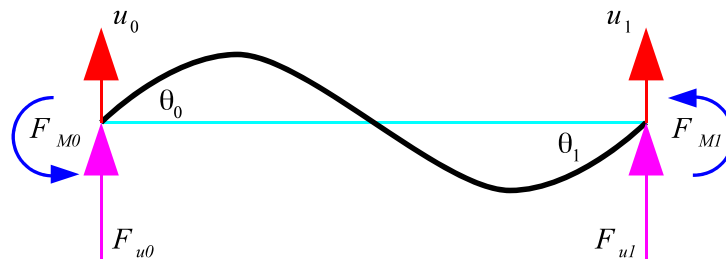


Figure D.2. Sign convention for the beam element [Haque, 2016]

The stiffness matrix is computed required to the general solutions of the equations for the beam.

The governing equation for a FEM of a beam is

$$[\mathbf{k}]\{\mathbf{u}\} = \{\mathbf{f}\} \quad (\text{D.7})$$

Where the stiffness matrix, $[\mathbf{k}]$, for a beam element is a 4×4 matrix. The displacements is described in the $\{\mathbf{u}\}$ vector, the load is applied in vector $\{\mathbf{f}\}$. Equation (D.7) can also be formulated as

$$\begin{bmatrix} k_{11} & k_{21} & k_{31} & k_{41} \\ k_{12} & k_{22} & k_{32} & k_{42} \\ k_{13} & k_{23} & k_{33} & k_{43} \\ k_{14} & k_{24} & k_{34} & k_{44} \end{bmatrix} \begin{Bmatrix} u_0 \\ \theta_0 \\ u_1 \\ \theta_1 \end{Bmatrix} = \begin{Bmatrix} F_{u_0} \\ F_{M_0} \\ F_{u_1} \\ F_{M_1} \end{Bmatrix}$$

To determine the different components of $[\mathbf{k}]$ the j -th column is considered. f_i is the applied forces necessary to a unit displacement $u_j = 1$ while the other displacements remain zero at the same time. The procedure to evaluate the j -th column of $[\mathbf{k}]$ is as follows

- Solving equations (D.2)-(D.5) with the boundary conditions as

$$u_i = \delta_{ij} = \begin{cases} 1 & \text{if } i = j \\ 0 & \text{if } i \neq j \end{cases}$$

- Determine the end moments M_0 , M_1 and the end shears V_0 , V_1 from the beam equations.
- The sign convention from the beam is translated to the element sign convention with:

$$K_{1_j} = V_0, \quad K_{2_j} = -M_0, \quad K_{3_j} = -V_1, \quad K_{4_j} = M_1$$

This procedure will be used in the next part of this report [Haque, 2016].

Construction of stiffness matrix

The stiffness matrix is constructed using the procedure described above. The first column in the matrix is determined by setting the unit displacement at the left end equal to one, this is illustrated at Figure D.3.

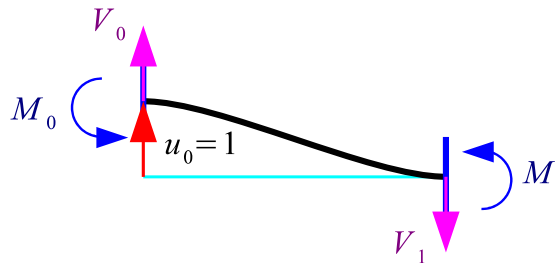


Figure D.3. Unit displacement $u_0 = 1$ [Haque, 2016]

As Figure D.3 shows is the BC $u_0 = 1$, $\theta_0 = 0$, $u_1 = 0$, $\theta_1 = 0$. Solving for $M_0 = 0$ in equation (D.4) knowing $\theta(L) = 0$, this gives

$$M_0 = -\frac{LV_0}{2}$$

Using this in equation (D.5) and $u_1 = 0$

$$\begin{aligned}
 0 &= \frac{L^3 V_0}{6EI} - \frac{L^3 V_0}{4EI} - \frac{LV_0}{GA_s} + 1 \\
 0 &= -\left(\frac{L^3}{12EI} + \frac{L}{GA_s}\right) V_0 + 1 \\
 1 &= \frac{L^3}{12EI} \left(1 + \frac{12EI}{L^2 GA_s}\right) V_0
 \end{aligned} \tag{D.8}$$

By using Φ as in equation (D.9) and substituting it into equation (D.8), gives equation (D.10)

$$\Phi = \frac{12EI}{L^2 GA_s} \tag{D.9}$$

$$V_0 = \frac{12EI}{L^3} (1 + \Phi)^{-1} \tag{D.10}$$

This gives that the moments at the ends are

$$\begin{aligned}
 M_0 &= -\frac{6EI}{L^2} (1 + \Phi)^{-1} \\
 M_1 &= \frac{6EI}{L^2} (1 + \Phi)^{-1}
 \end{aligned}$$

The sign convention of the beam is translated to matrix sign convention and the first column of the stiffness matrix is

$$\begin{bmatrix} K_{11} \\ K_{21} \\ K_{31} \\ K_{41} \end{bmatrix} = \begin{bmatrix} V_0 \\ -M_0 \\ -V_1 \\ M_1 \end{bmatrix} = \frac{EI}{(1 + \Phi)L^3} \begin{bmatrix} 12 \\ 6L \\ -12 \\ 6L \end{bmatrix}$$

The second column is determined with setting the rotation at the left end equal to one as shown in Figure D.4

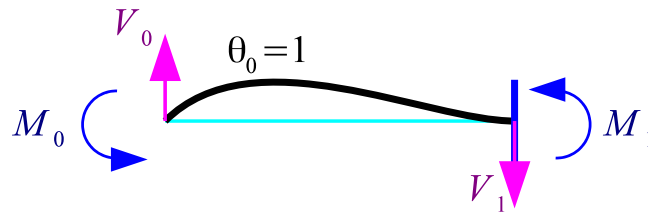


Figure D.4. Unit displacement $\theta_0=1$ [Haque, 2016]

As Figure D.4 shows is the BC now $u_0 = 0$, $\theta_0 = 1$, $u_1 = 0$, $\theta_1 = 0$. Solving for $M_0 = 0$ in equation (D.5) knowing $u(L) = 0$, this gives

$$M_0 = -\frac{LV_0}{2} - \frac{EI}{L}$$

Using this in equation (D.5) and with some mathematical use this gives

$$V_0 = \frac{6EI}{L^2} (1 + \Phi)^{-1}$$

Where Φ is the same as in equation (D.9). This is used to determine the moments at the ends, this is done as

$$\begin{aligned} M_0 &= -\frac{3EI}{L}(1 + \Phi)^{-1} - \frac{EI}{L} \\ M_0 &= -\frac{3EI}{L}(1 + \Phi)^{-1} - \frac{EI}{L}(1 + \Phi)(1 + \Phi)^{-1} \\ M_0 &= -\frac{EI}{L}(4 + \Phi)(1 + \Phi)^{-1} \\ M_1 &= LV_0 + M_0 \\ M_1 &= \frac{6EI}{L}(1 + \Phi)^{-1} - \frac{EI}{L}(4 + \Phi)(1 + \Phi)^{-1} \\ M_1 &= \frac{EI}{L}(2 - \Phi)(1 + \Phi)^{-1} \end{aligned}$$

The second column of the stiffness matrix is described by translating the beam sign convention to matrix sign convention and the results is as

$$\begin{bmatrix} K_{12} \\ K_{22} \\ K_{32} \\ K_{42} \end{bmatrix} = \begin{bmatrix} V_0 \\ -M_0 \\ -V_1 \\ M_1 \end{bmatrix} = \frac{EI}{(1 + \Phi)L^3} \begin{bmatrix} 6L \\ (4 + \Phi)L^2 \\ -6L \\ (2 - \Phi)L^2 \end{bmatrix}$$

The third and fourth column in the stiffness matrix is made in the the same way. Figure D.5 is showing the boundary conditions for the third column while Figure D.6 shows them for the last column.

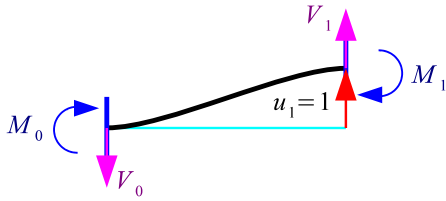


Figure D.5. Unit displacement $u_1=1$
[Haque, 2016]

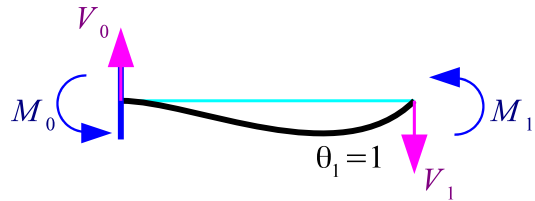


Figure D.6. Unit displacement $\theta_1=1$
[Haque, 2016]

Form these the last columns give

$$\begin{bmatrix} K_{13} \\ K_{23} \\ K_{33} \\ K_{43} \end{bmatrix} = \begin{bmatrix} V_0 \\ -M_0 \\ -V_1 \\ M_1 \end{bmatrix} = \frac{EI}{(1 + \Phi)L^3} \begin{bmatrix} -12 \\ -6L \\ 12 \\ -6L \end{bmatrix} \quad \begin{bmatrix} K_{14} \\ K_{24} \\ K_{34} \\ K_{44} \end{bmatrix} = \begin{bmatrix} V_0 \\ -M_0 \\ -V_1 \\ M_1 \end{bmatrix} = \frac{EI}{(1 + \Phi)L^3} \begin{bmatrix} 6L \\ (2 - \Phi)L^2 \\ -6L \\ (4 + \Phi)L^2 \end{bmatrix}$$

When all the columns for the stiffness matrix for the element are determined the matrix can be assembled as

$$[\mathbf{k}] = \frac{EI}{(1 + \Phi)L^3} \begin{bmatrix} 12 & 6L & -12 & 6L \\ 6L & (4 + \Phi)L^2 & -6L & (2 - \Phi)L^2 \\ -12 & -6L & 12 & -6L \\ 6L & (2 - \Phi)L^2 & -6L & (4 + \Phi)L^2 \end{bmatrix} \quad (\text{D.11})$$

This gives the following equilibrium equation

$$\frac{EI}{(1 + \Phi)L^3} \begin{bmatrix} 12 & 6L & -12 & 6L \\ 6L & (4 + \Phi)L^2 & -6L & (2 - \Phi)L^2 \\ -12 & -6L & 12 & -6L \\ 6L & (2 - \Phi)L^2 & -6L & (4 + \Phi)L^2 \end{bmatrix} \begin{Bmatrix} u_0 \\ \theta_0 \\ u_1 \\ \theta_1 \end{Bmatrix} = \begin{Bmatrix} F_{u_0} \\ F_{M_0} \\ F_{u_1} \\ F_{M_1} \end{Bmatrix}$$

D.1.3 Connecting elements

When connecting two elements stiffness matrices together the stiffness for the first element is combined with the stiffness of the second. The stiffness matrix for the combined elements is constructed by combining the stiffness in each node.

When considering a structure build of uniform elastic bars attached end to end only axial displacements are allowed. The stiffness of the respective elements are k_i [Cook et al., 2002].

An example of how to establish the combined stiffness matrix is made in the following. First is the figure of two bar elements shown and from this figure the combined stiffness matrix will be established.

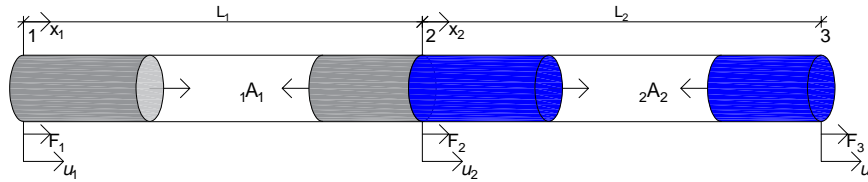


Figure D.7. Bar elements connected together end to end

From the equilibrium conditions for node 1

$$\sigma_1 A_1 + F_1 = E_1 A_1 \varepsilon_1 + F_1 = \frac{E_1 A_1}{L_1} (u_2 - u_1) + F_1 = 0 \Rightarrow$$

$$k_1 u_1 - k_1 u_2 = F_1 ; k_1 = \frac{E_1 A_1}{L_1}$$

From the equilibrium conditions for node 2

$$-\sigma_1 A_1 + \sigma_2 A_2 + F_2 = -\frac{E_1 A_1}{L_1} (u_2 - u_1) + \frac{E_2 A_2}{L_2} (u_3 - u_2) + F_2 = 0 \Rightarrow$$

$$-k_1 u_1 + (k_1 + k_2) u_2 - k_2 u_3 = F_2 ; k_1 = \frac{E_1 A_1}{L_1} ; k_2 = \frac{E_2 A_2}{L_2}$$

From the equilibrium conditions for node 3

$$-\sigma_2 A_2 + F_3 = -E_2 A_2 \varepsilon_2 + F_3 = -\frac{E_2 A_2}{L_2} (u_3 - u_2) + F_3 = 0 \Rightarrow$$

$$-k_2 u_2 + k_2 u_3 = F_3 ; k_2 = \frac{E_2 A_2}{L_2}$$

Equilibrium conditions for all nodes

$$\text{At node 1: } k_1 u_1 - k_1 u_2 = F_1$$

$$\text{At node 2: } -k_1 u_1 + (k_1 + k_2) u_2 - k_2 u_3 = F_2$$

$$\text{At node 3: } -k_2 u_2 + k_2 u_3 = F_3$$

This can be expressed on matrix form as

$$\begin{bmatrix} k_1 & -k_1 & 0 \\ -k_1 & k_1 + k_2 & -k_2 \\ 0 & -k_2 & k_2 \end{bmatrix} \begin{Bmatrix} u_1 \\ u_2 \\ u_3 \end{Bmatrix} = \begin{Bmatrix} F_1 \\ F_2 \\ F_3 \end{Bmatrix} \quad \text{with} \quad k_1 = \frac{E_1 A_1}{L_1}; \quad k_2 = \frac{E_2 A_2}{L_2}$$

On Finite element form

$$[\mathbf{K}] \{\mathbf{D}\} = -\{\mathbf{R}\}$$
$$[\mathbf{K}] = \begin{bmatrix} k_1 & -k_1 & 0 \\ -k_1 & k_1 + k_2 & -k_2 \\ 0 & -k_2 & k_2 \end{bmatrix}; \quad \{\mathbf{D}\} = \begin{Bmatrix} u_1 \\ u_2 \\ u_3 \end{Bmatrix}; \quad \{\mathbf{R}\} = -\begin{Bmatrix} F_1 \\ F_2 \\ F_3 \end{Bmatrix}$$